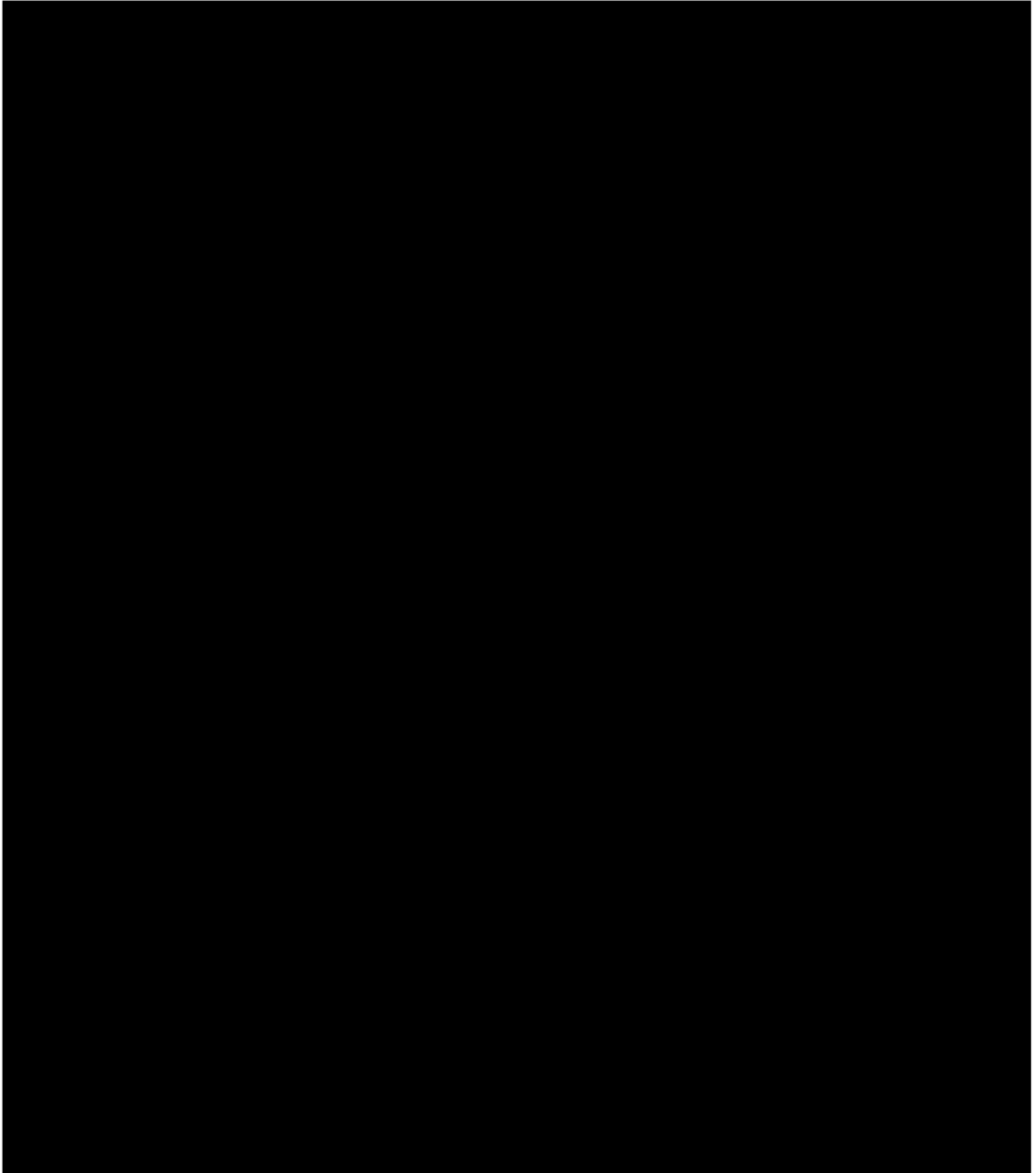


# AIRBUS SLOSHING ROCKET WORKSHOP

2024 EDITION



# Table of Contents

Table of Figures .....	5
Acknowledgements .....	6
Abstract.....	7
Notation .....	8
Abbreviations .....	8
1. Introduction.....	9
1.1 Review of the sloshing subject.....	9
Challenge of sloshing liquid propellants in the aerospace industry .....	9
Interesting and innovative ideas aviation should take inspiration from .....	9
1.2 Team organization .....	10
2. Design Requirements .....	11
2.1. General.....	11
2.2. Summary of requirements.....	11
3. Concept Design .....	12
4. General Design Arrangement .....	12
3D Model Renders.....	13
Technical Drawings.....	15
5. Propulsion .....	16
5.1 General.....	16
5.2 PTES .....	16
Simulation .....	16
Assumptions.....	17
5.3 Results .....	18
Simulation 1 – Variable Pressure .....	18
Simulation 2 – Variable Volume .....	19
Simulation 3 – Variable Empty Mass .....	19
Simulation 4 – Variable Filling Factor .....	20
5.4 Launch System.....	20
Design .....	20
Render.....	21
Technical Drawing .....	21
Manufacturing.....	22
Testing.....	23
6. Aerodynamics .....	24

6.1 General.....	24
6.2 Tail Fins Design .....	24
Technical Drawing .....	24
6.3 Tail Fins Manufacture.....	25
6.4 Main Wings .....	26
Airfoil.....	26
Wing Design .....	28
Technical Drawing .....	28
Deployment Mechanism .....	28
6.5 CFD Simulations .....	29
Assumptions .....	29
Results .....	29
6.6 Wing Manufacturing.....	31
7. Simulators - Flight Modelling .....	32
7.1 FDPS .....	32
Assumptions.....	32
7.2 Results .....	33
Inputs .....	33
Deployable Wings Advantage .....	34
Outputs .....	34
8. Sloshing Management – Tank Design.....	38
General .....	38
Damping Mechanism .....	38
Tank Design .....	39
Manufacturing .....	39
Simulation.....	40
Assumptions .....	41
9. Structural Design .....	42
9.1 Materials.....	42
9.2 Main Load Bearing Structure .....	42
FEA.....	42
9.3 Nose Cone .....	43
9.4 Main Wings .....	43
9.5 Propulsion Tank.....	43
9.6 3D-Printed parts .....	44

10. Control.....	44
11. Bill of Materials .....	45
12. Risk Assessment.....	47
Conclusion .....	48
Appendix.....	49
FDPS Matlab Code .....	49
PTES Matlab Code.....	52
Matlab Simulink Model.....	55
Arduino Code for Barometric Sensor .....	56
Bibliography .....	57

## Table of Figures

Figure 2.1: Simulator modelling flow .....	11
Figure 4.1: 3D model Isometric View .....	13
Figure 4.2: 3D model Isometric View 2 .....	13
Figure 4.3: Breakout Side Section View.....	14
Figure 4.4: Technical Drawing - Wings Stowed.....	15
Figure 4.5: Technical Drawing - Wings Deployed.....	15
Figure 5.1: Thrust efficiency for different pressures .....	18
Figure 5.2: Thrust efficiency for different volumes .....	19
Figure 5.3: Thrust efficiency for different empty mass .....	19
Figure 5.4: Thrust Efficiency for constant parameters .....	20
Figure 5.5: 3D model of Launch System .....	21
Figure 5.6: Technical Drawing of Launch System .....	21
Figure 5.7: Photo of launch system inlet.....	22
Figure 5.8: Launch System Pressure testing.....	23
Figure 5.9: Launch System Leakage Testing.....	23
Figure 6.1: Tail fins Technical Drawing .....	24
Figure 6.2: Photo 1 of 3D Printed Tail Fin .....	25
Figure 6.3: Photo 2 of 3D Printed Tail Fin .....	25
Figure 6.4: Technical Drawing of Main Wing.....	28
Figure 6.5: Velocity Field Top View (Wings Stowed) .....	29
Figure 6.6: Velocity Field Side View (Wings Stowed) .....	29
Figure 6.7: Velocity Field Side View (Wings Deployed) .....	30
Figure 6.8: Velocity Field Top View (Wings Deployed) .....	30
Figure 6.9: Foam Cutting Guide Rails .....	31
Figure 6.10: Finished Wings.....	31
Figure 7.1: Inputs in external burnout data calculator .....	33
Figure 7.2: Flight Profile graph without deployable wings system .....	34
Figure 7.3: Flight profile graph with deployable wings system .....	34
Figure 7.4: Flight profile graph .....	34
Figure 7.5: Altitude – Range graph .....	35
Figure 7.6: Vertical – Lateral Speed graph.....	35
Figure 7.7: Pitch angle – Time graph .....	36
Figure 7.8: Horizontal – Vertical Acceleration graph .....	36
Figure 7.9: Drag – Lift Graph .....	37
Figure 8.1: Damping as a function of flexibility F [STEPHENS & SCHOLL, 1967].....	38
Figure 8.2: Tank Breakout View .....	39
Figure 8.3: 3D Printed Flexible Baffle .....	39
Figure 8.4: Fluid motion without baffle at 1.35s .....	40
Figure 8.5: Fluid motion without baffle at 1.5s .....	40
Figure 8.6: Fluid motion with baffle at 1.35s .....	41
Figure 8.7: Fluid motion with baffle at 1.5s .....	41
Figure 9.1: FEA Results (Displacement).....	43
Figure 9.2: Tri-hexagon pattern <sup>[8]</sup> .....	44
Figure 10.1: Radio Control Module.....	44
Figure 11.1: Prototype.....	46

## Acknowledgements

I, [REDACTED], would like to thank my team for their cooperation and excellent teamwork. In addition, I would like to thank my father for being a continuous inspiration and for his help with designing and making the aircraft.

In addition, the project would not have been made possible without the help of [REDACTED] in operating the OpenFOAM software to produce the sloshing simulations. A [REDACTED] contributions were fundamental to shaping the wings as well as making the foam cutter. I want to acknowledge the contributions of [REDACTED] and [REDACTED] providing the necessary equipment and tooling to shape the wings. Finally, I would like to thank [REDACTED] for reviewing the present technical report.

The following software were used in the project:

- [Autodesk Fusion](#)
- [Autodesk CFD](#)
- [Mathworks Matlab](#)
- [Mathworks Simulink](#)
- [Arduino IDE](#)
- [OpenFOAM](#)

## Abstract

This technical report is the official entry of the team [REDACTED] into the Airbus Sloshing Rocket Workshop 2024 Competition. This report presents the findings and methodologies of the teams' effort, focusing on the dynamics of fluid sloshing in aerospace applications. Through a combination of computational simulations, experimental analyses, and theoretical modeling, the team explored various strategies to mitigate sloshing effects and develop a stable aircraft platform. Key outcomes include the development of passive damping systems, optimized simulations, and improved predictive models. Finally, the report aims to provide insight into how simulation driven design choices can help increase efficiency of aircraft and space vehicles experiencing sloshing loads.

## Notation

<i>Symbol</i>	<i>Description</i>
$P$	Pressure
$V$	Volume
$T$	Temperature
$\rho$	Air Density
$\rho_{water}$	Water Density
$\gamma$	Heat capacity ratio
$f$	Filling ratio
$m$	Empty Mass
$S$	Wing Area
$u_{\infty}$	Free stream velocity
$Cl$	Lift Coefficient
$C_{D_{stowed}}$	Drag Coefficient (Wings Stowed)
$C_{D_{deployed}}$	Drag Coefficient (Wings Deployed)

## Abbreviations

AOA: Angle of Attack

FDPS: Flight Dynamics and Performance Simulator

PTES: Propulsion and Thrust Efficiency Simulator

CFD: Computational Fluid Dynamics

FEA: Finite Element Analysis

TOW: Take Off Weight

MDF: Medium Density Fiberboard



# 1. Introduction

## 1.1 Review of the sloshing subject

### Challenge of sloshing liquid propellants in the aerospace industry

In the aerospace industry liquids are frequently involved in various roles, including propulsion, ballast, control means for systems, means of cooling and as payload. Examples include liquid fuel, hydraulic fluids and liquid cooling agents. Storing and utilizing these liquids can be a challenge under accelerations and unpredictable movements that are unavoidable during flight activities. All these challenges involving liquids can be primarily described by the term *liquid sloshing*. *Liquid sloshing* or just *sloshing* refers to the movement of liquid within an enclosed container. In the context of aerospace, sloshing can significantly impact flight dynamics and stability. Specifically, the main problems regarding sloshing in the aerospace field:

- Aircraft fuel sloshing

Fuel sloshing occurs in aircraft fuel tanks during flight. As the aircraft maneuvers sloshing is introduced due to the liquid nature of the fuel. This effect has an impact in flight stability as the movement of the fuel causes a shift in center of gravity, that can in turn impact the longitudinal stability of the aircraft.

- Spacecraft propellant sloshing

In space vehicles, propellant sloshing can alter the dynamics of space vehicles as described above but can also impact the consistency of propellant flow into the engines or even prevent propellant from reaching the engines completely.

In summary, sloshing affects both aircraft and spacecraft, necessitating careful design and management to ensure safety and stability during flight and space missions.

### Interesting and innovative ideas aviation should take inspiration from

There are many interesting ideas aviation should explore. As always, nature can inspire ideas for the challenges discussed above. Specifically, these are some interesting mechanisms or phenomena:

- Viscous Damping in Wetlands

In wetlands and marshes, vegetation and submerged obstacles create viscous damping. As water flows through these areas, the frictional resistance from plants and obstacles slows down and restricts water movement. In engineering that translates to advanced *flexible baffle* designs that can contribute to sloshing damping.

- Surface Tension effects

Some insects like the Gerridae utilize surface tension effects to move on water surfaces. In a similar way surface tension can be exploited to restrict liquid movement, through coatings or *surface treatments* inside the walls of tanks that increase the resistance in the liquid's movement. This can in turn mitigate sloshing effects.

## 1.2 Team organization

Our team, [REDACTED] consists of 3 members, all of whom are undergraduate students in the [REDACTED]. The team is joined by a common passion for aviation and tackling engineering challenges.

Below are the members of the team:

Team Leader, responsible for the team coordination, construction supervision and design analysis. Contributions to the project:

- Simulators
- CFD
- FEA
- Propulsion specialist
- Aircraft characteristic analysis
- Aerodynamics Design

Team member, responsible for the construction and design of the aircraft. Contributions to the project:

- Construction specialist
- Avionics specialist
- Controls specialist
- Structural Design

Team member, responsible for compliance with rules and regulations. Contributions to the project:

- Technical report proof checking
- Rules compliance check
- Research

## 2. Design Requirements

### 2.1. General

Design requirements guided the whole project and the design of the aircraft. In order to find the parameters that affect the performance of the aircraft and to measure the impact of each parameter two custom simulators were developed.

The simulators were initially provided with estimations and rough guesses and through many iterations more accurate results were acquired that were fed into the simulators again, each time reducing the uncertainty of the parameters involved.

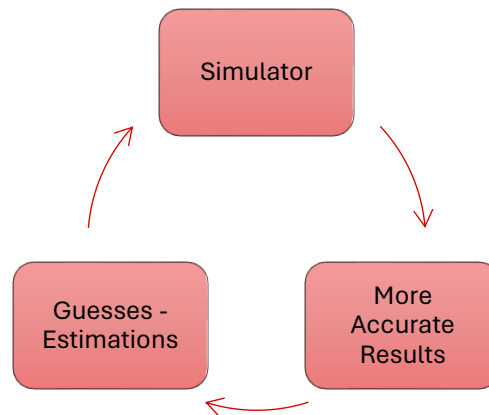


Figure 2.1: Simulator modelling flow

Afterwards a sensitivity analysis was performed varying iteratively the parameter values and using the score formula (see below) provided different scores were calculated, providing a measure of the performance of the rocket.

$$Score = \frac{distance \cdot time \cdot payload}{TOW}$$

The sensitivity analysis resulted in the following table of design requirements, where both a threshold (lowest acceptable performance) and a target (ideal performance) was set.

### 2.2. Summary of requirements

Requirement	Threshold	Target
Range	>5m	20m
Peak Altitude	>10m	15m
Stall Speed	<5m/s	3m/s
Payload Mass	>0.5kg	0.75kg
Empty Mass	<0.7kg	0.3kg
Controllability	Radio Controlled: <ul style="list-style-type: none"><li>Pitch</li></ul>	Fully Autonomous: <ul style="list-style-type: none"><li>Pitch</li><li>Yaw</li><li>Roll</li></ul>

Table 2.1: Design Requirements

### 3. Concept Design

The concept design phase required extensive research and concept evaluations, in order to maximize the performance of the aircraft and to make sure that the aircraft can be manufactured easily and inexpensively.

The design of the aircraft focused on maximizing the range after launch and achieving the target payload of 0.75kg. Therefore, a foldable wing setup was developed, and attention was given in shaping the aircraft to reduce aerodynamic drag during launch. The aircraft will launch with the wings stowed and deploy the wings automatically upon reaching the peak altitude, resulting in increased range and shallower descend angles. It will feature yaw and pitch remote control and will record data for post-flight analysis through a set of avionics and sensors.

#### 4. General Design Arrangement

In this section the general placement of parts and systems is described. The aircraft consists of the following parts:

[illegible]

Table 4.1: Aircraft Parts

The 3D model renderings of the aircraft are shown on the next page.

## 3D Model Renders

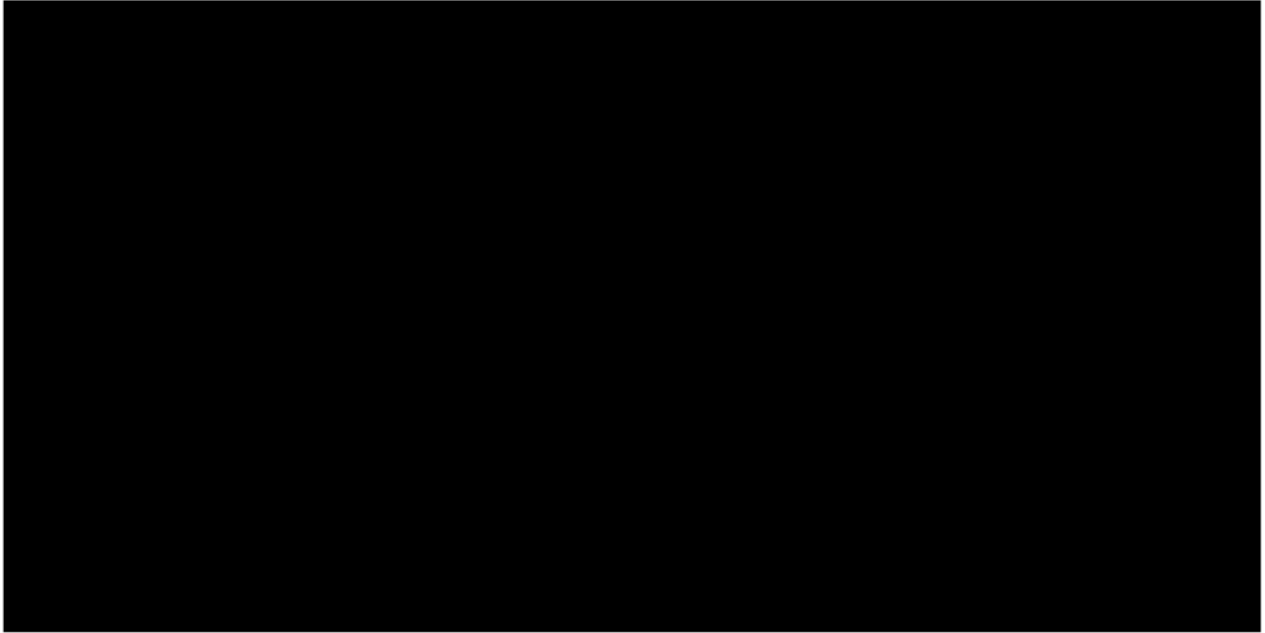


*Figure 4.1: 3D model Isometric View*

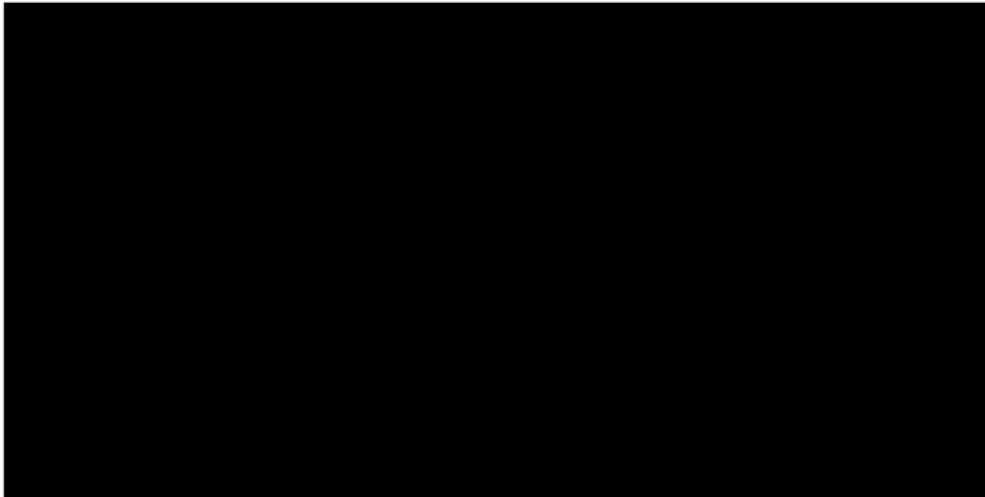


*Figure 4.2: 3D model Isometric View 2*



*Figure 4.3: Breakout Side Section View*

## Technical Drawings

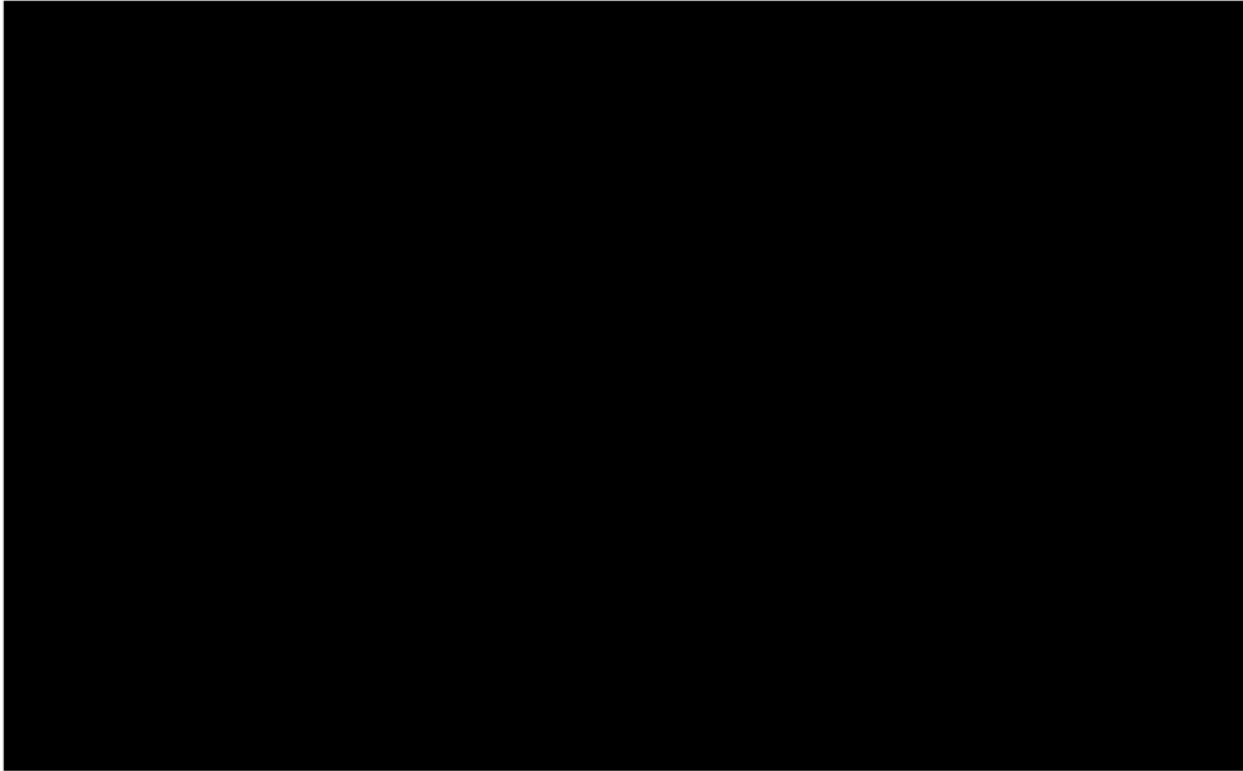


*Figure 4.4: Technical Drawing - Wings Stowed*

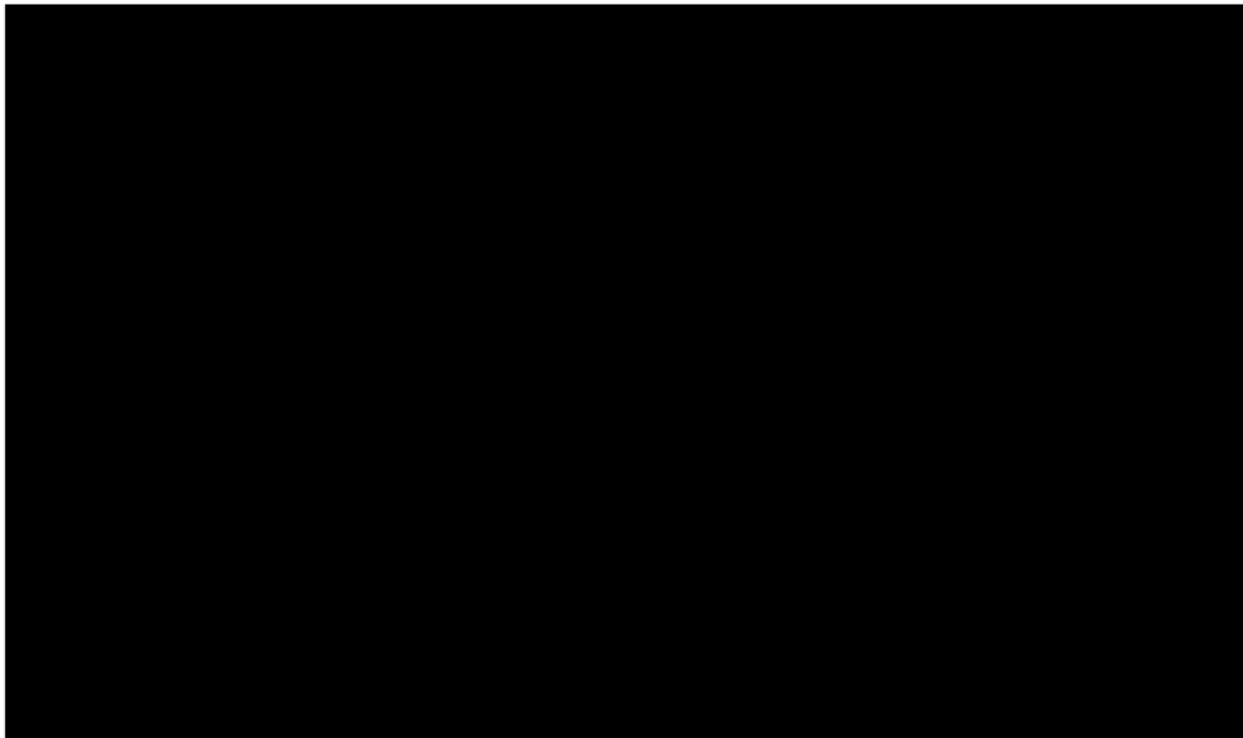


*Figure 4.5: Technical Drawing - Wings Deployed*

## 5. Propulsion

### 5.1 General

The launching mechanism is required to be able to provide adequate pressurized air to the aircraft in order to launch it. The final stage of the launch mechanism that goes into the aircraft propulsion tank, known as the launch tube, is also required to be tilted at 85 degrees. For the assembly copper tubes were selected for their ease of joining and durability under high pressures. Finally, a release pin allows for safe and quick launches by separating the aircraft from the launch tube.

### 5.2 PTES

#### Simulation

The **Propulsion and Thrust Efficiency Simulator (PTES)** gets environmental parameters and launch-setup data in order to provide the best launch settings, the outputs are:

- Ideal Pressure
- Ideal Volume
- Ideal Empty Mass

The PTES is based on the following principles<sup>[2]</sup>. The thrust of the water-propulsion system can be attributed to two different phenomena; the first is the rapidly exiting water and the second is the exit of the remaining compressed air after the depletion of water.

The work done by the gas in an incremental expansion is:

$$W = \int_{initial\ volume}^{final\ volume} P dV \quad (1)$$

The expansion the gas is rapid enough to be considered adiabatic, and so conforms to the law:

$$PV^\gamma = K \quad (2)$$

where  $K$  is a constant. So, the work done in the expansion is:

$$W = \int_{initial\ volume}^{final\ volume} \frac{K}{V^\gamma} dV = K \cdot \left[ \frac{V^{-\gamma+1}}{-\gamma+1} \right]_{initial\ volume}^{final\ volume} = K \cdot \left[ \frac{V_{final}^{-\gamma+1}}{-\gamma+1} \right] - K \cdot \left[ \frac{V_{initial}^{-\gamma+1}}{-\gamma+1} \right] = \frac{K}{-\gamma+1} \cdot [V_{final}^{-\gamma+1} - V_{initial}^{-\gamma+1}] \quad (3)$$

The final volume is the simply the full volume of the tank,  $V$ . The initial volume is  $(1 - f) \cdot V$  where  $f$  is the filling fraction of the tank.

$$W = \frac{KV^{-\gamma+1}}{-\gamma+1} [V^{-\gamma+1} - V^{-\gamma+1} \cdot (1 - f)^{-\gamma+1}] = \frac{KV^{-\gamma+1}}{-\gamma+1} \cdot [1 - (1 - f)^{-\gamma+1}] \quad (4)$$

The value of  $K$  is determined by the initial conditions in equation (2):

$$K = P \cdot (1 - f)^\gamma \cdot V^\gamma \quad (5)$$

From (5) and (4):

$$W = \frac{P \cdot V}{-\gamma+1} \cdot [(1 - f)^\gamma - (1 - f)] \quad (6)$$

The simulator calculates the specific work by dividing the formula (6) with mass, allowing for accurate efficiency calculations regarding, initial pressure and filling factors.



## Assumptions

In the modelling process the team made certain assumptions. This section lists the assumptions made and their possible implications on the simulation results.

### Environmental parameters

1. No wind effects are taken into account.
2. Heat capacity ratio is taken as  $\gamma = 1.4$ .
3. The **International Standard Atmosphere**<sup>[5]</sup> model was used, specifically:
  - Temperature is considered constant at  $T = 288K$ .
  - Pressure is considered constant at  $P = 101,325 Pa$ .
  - Atmospheric density is considered constant at  $\rho = 1.225 \frac{kg}{m^3}$

### Propulsion Analysis

1. The expansion of the propulsion gases is considered adiabatic.
2. The water's density inside the tank was taken as  $\rho_{water} = 997 \frac{kg}{m^3}$

### 5.3 Results

For the sensitivity and parameter-impact analysis, each couple of parameters were “frozen” at a specific value while the work produced, and the filling factor were continuously varying. The following table shows the “frozen” values for each parameter.

Parameter	Value
Pressure ( $P$ )	$7 \cdot 10^5 \text{ Pa}$
Tank Volume ( $V$ )	$1.5 \cdot 10^{-3} \text{ m}^3$
Empty Mass ( $m$ )	$0.6 \text{ kg}$

Table 5.1

#### Simulation 1 – Variable Pressure

##### Efficiency for different Pressures

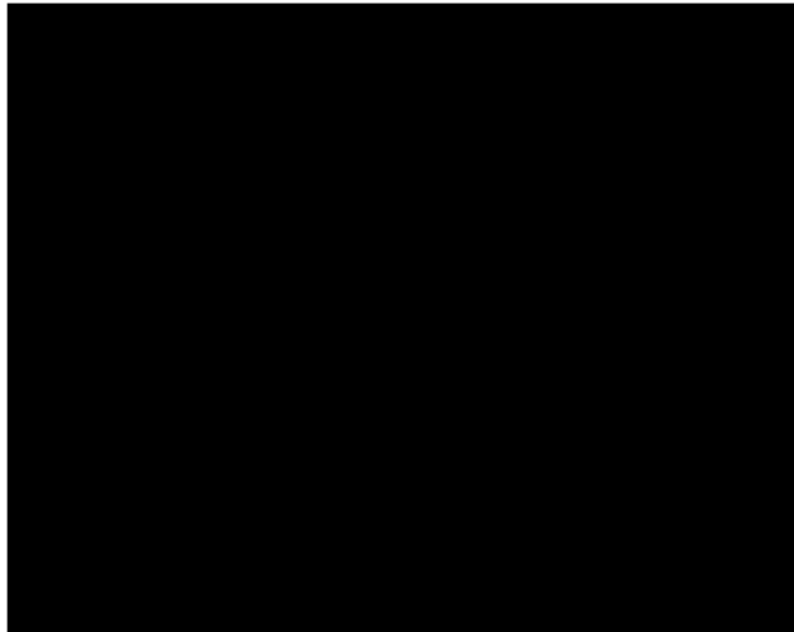
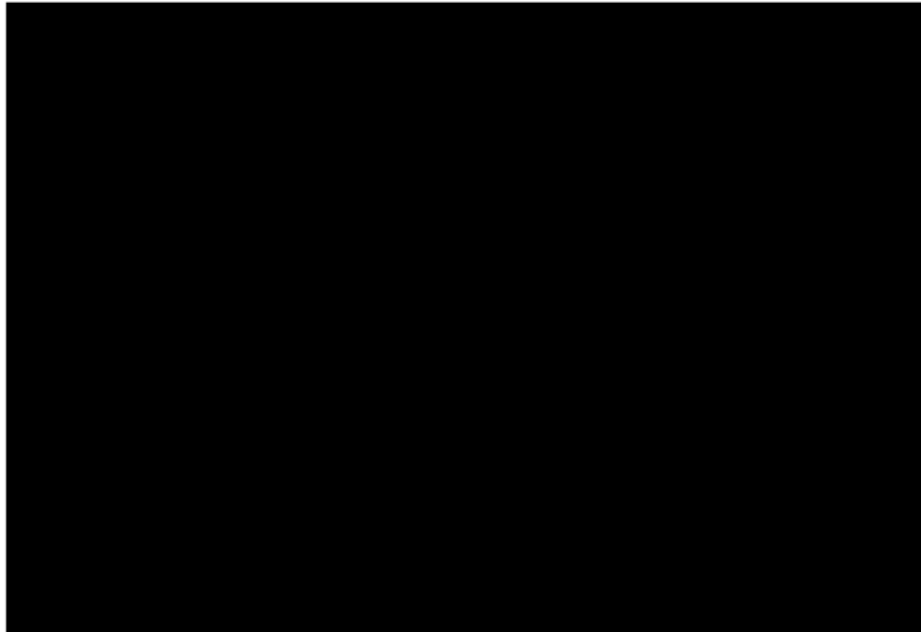


Figure 5.1: Thrust efficiency for different pressures

From this simulation it is easily determined that the relation between pressure and work is (as expected) linear. This means that at launch the propulsion system needs to have the maximum allowed pressure. For safety reasons and air pump equipment limitations the team decided to aim for a pressure of 7bar ( $7 \cdot 10^5 \text{ Pa}$ ) with the possibility of increasing the pressure in the future to 9bar (10 bar is maximum pressure according to the regulations).

## Simulation 2 – Variable Volume

### Efficiency for different Volume



*Figure 5.2: Thrust efficiency for different volumes*

From this simulation the work is again linearly dependent on the tank volume. Due to the propulsion tank being an off-the-shelf item (soda bottle) the only realistic options were 0.5, 1 and 1.5-Liter bottles of which the 1.5 Liter bottle was selected for its superior performance.

## Simulation 3 – Variable Empty Mass

### Efficiency for different Empty Mass

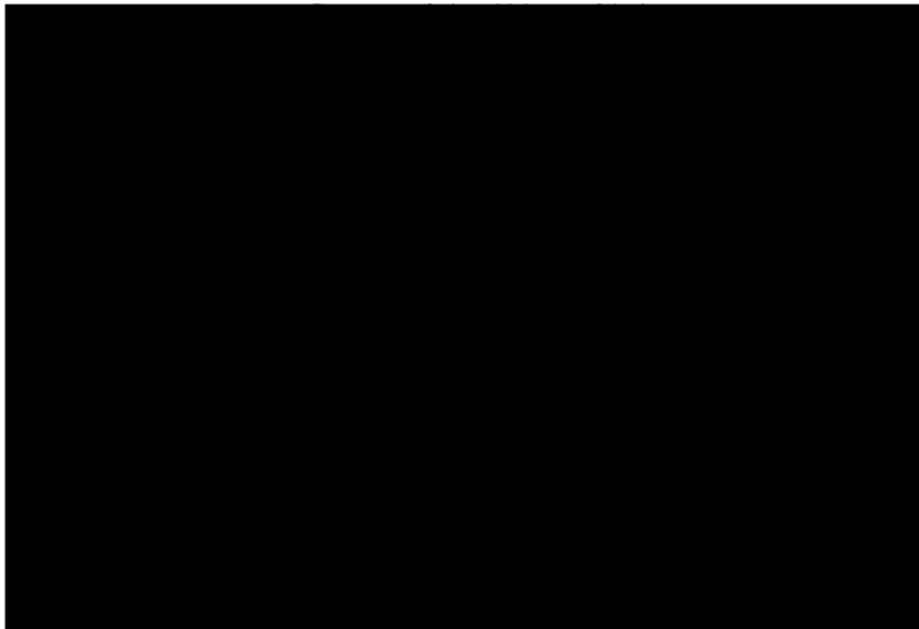


*Figure 5.3: Thrust efficiency for different empty mass*

From this simulation, it is evident that empty mass is the most sensitive of the previous parameters, since a small change impacts the work done greatly. Therefore, the design of the rocket and specifically the structural design prioritized low mass structures to achieve the best performance.

#### Simulation 4 – Variable Filling Factor

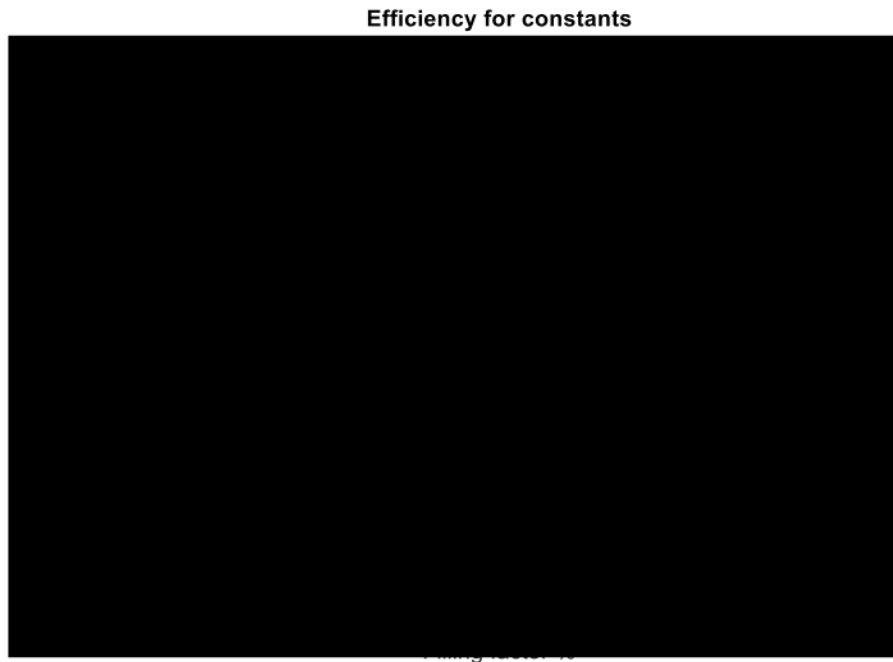


*Figure 5.4: Thrust Efficiency for constant parameters*

The final simulation resulted in the best filling factor for optimal performance, with all other variables constant with the values of table 3. The best filling factor was determined to be **40%**, resulting in 0.6Liters of propellant water.

## 5.4 Launch System

### Design

In this section the design of the launch system is described. The launch system consists of the following parts:

Part Numbering	Part Name

*Table 5.2*

Render

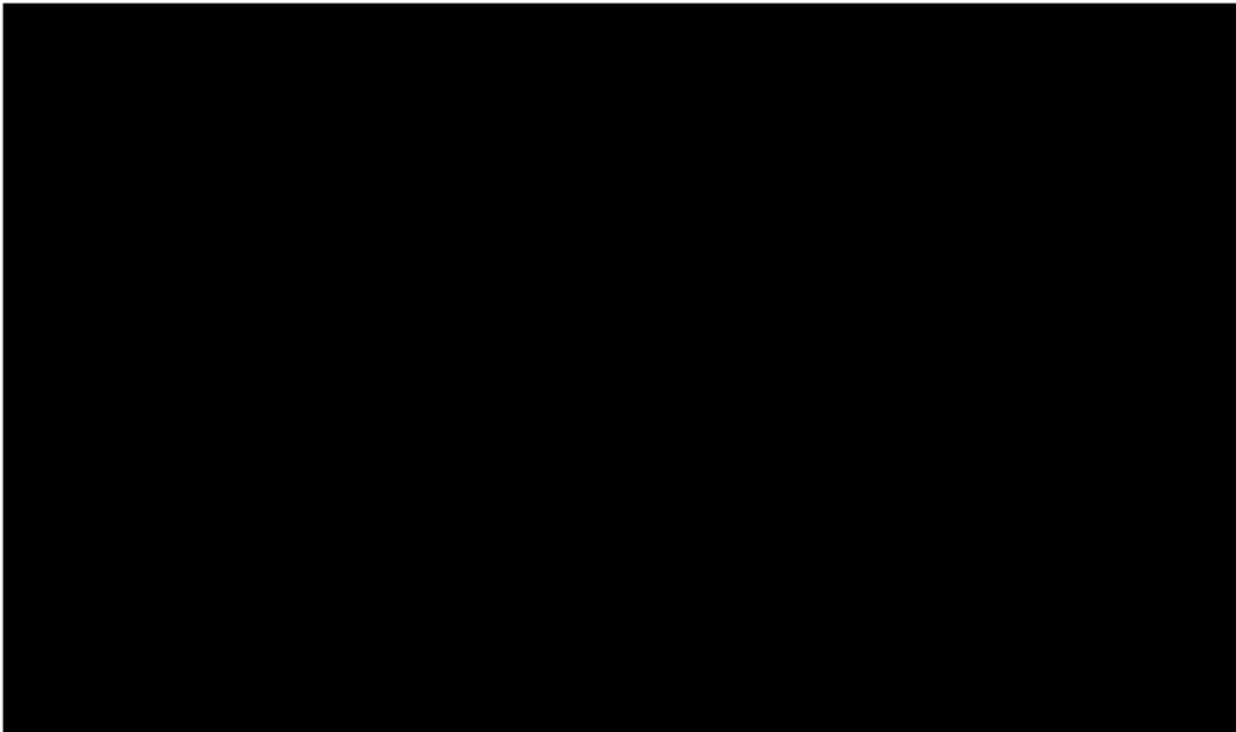


*Figure 5.5: 3D model of Launch System*

Technical Drawing

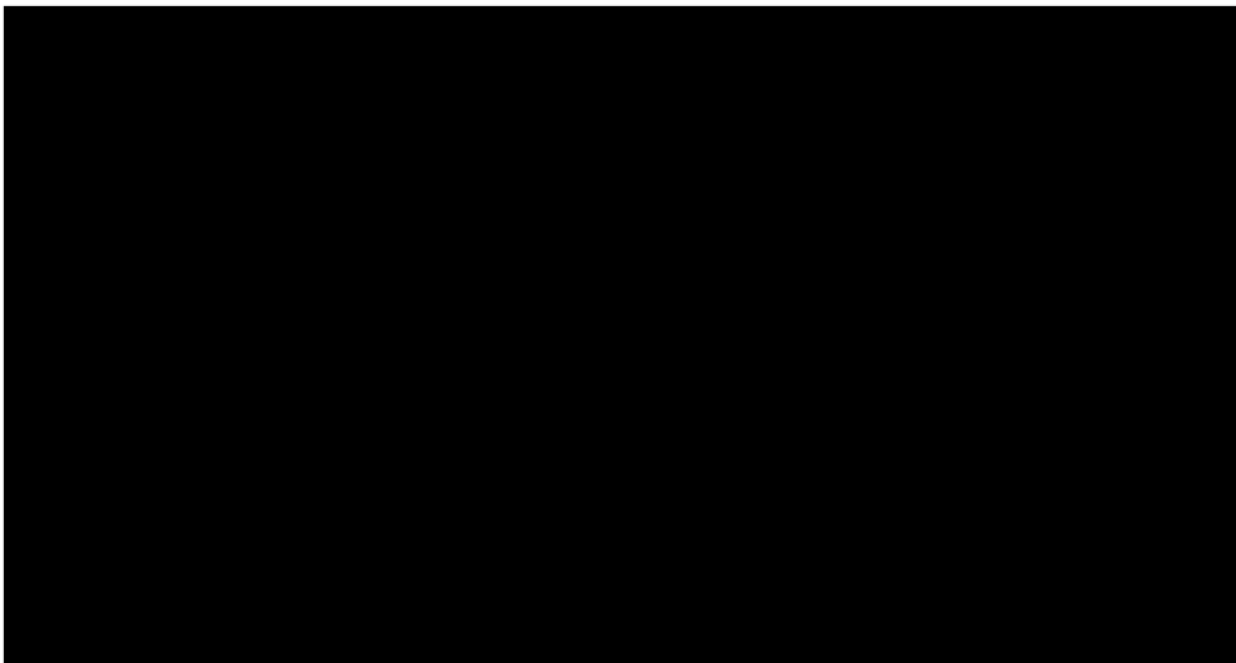


*Figure 5.6: Technical Drawing of Launch System*

## Manufacturing

The manufacturing of the launch system included cutting the copper tube at specified lengths, assembling the parts, and welding them together to ensure adequate sealing.

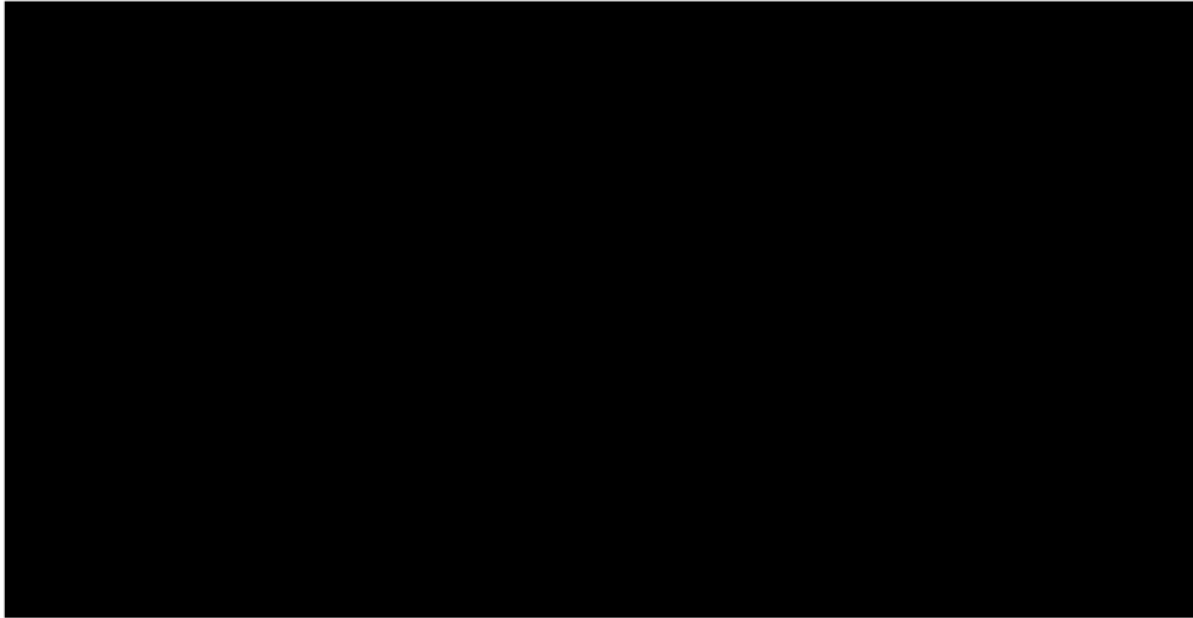


*Figure 5.7: Photo of launch system inlet*

## Testing

The launch system was tested to ensure that the design would withstand the pressure, without leaking. It was tested in the following ways:

- Pressure Testing
- Leakage Testing

### Pressure Testing

The open end of the launch tube was sealed, and pressure was incrementally applied. Initially, 5 bar of pressure was applied to the tube for 5 minutes and afterwards 7bar of pressure was applied for a duration of 1 hour. Both tests were successful, as the valve closed normally, and no structural buckling was observed.

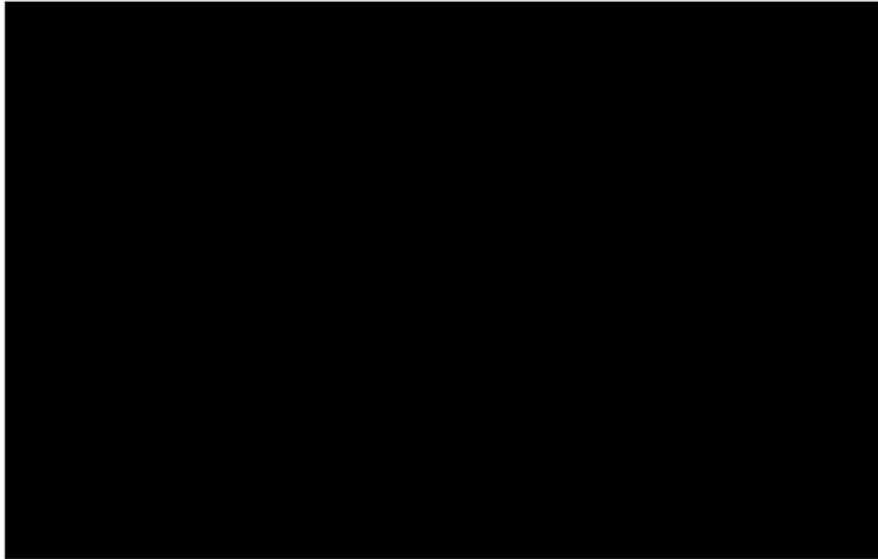


*Figure 5.8: Launch System Pressure testing*

### Leakage Testing

At a pressure of 7 bar the launch system was placed in water to check for leaks at all the welds and joints. The test was completed successfully as no air escaped.

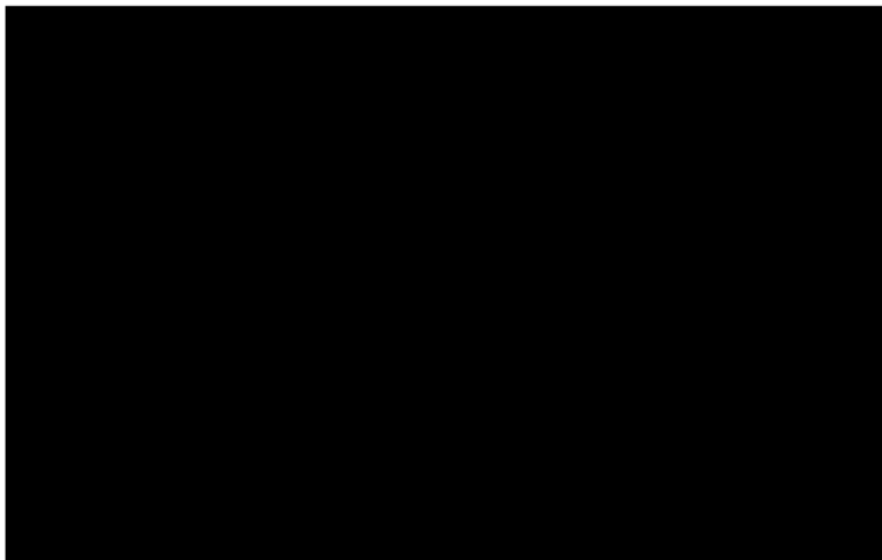


*Figure 5.9: Launch System Leakage Testing*

## 6. Aerodynamics

### 6.1 General

Aerodynamics design was focused on minimizing drag on the ascend phase and maximizing lift during the descend stage of the aircraft. This was achieved through a foldable wing system. Passive aerodynamic stability was also researched resulting in changes in airfoil, wing position and wing sweep angle.

### 6.2 Tail Fins Design

A triple fin tail section was implemented to allow for control of pitch and yaw of the aircraft. The tail fins are designed to have the least amount of induced drag while still being able to provide adequate control authority when the control surfaces are deflected.

The airfoil selected was a [REDACTED]. The airfoil was made elliptical to reduce induced drag. The control surface is placed into the wing with an axle allowing for deflection. The chord length was chosen as [REDACTED] to enhance the characteristics of the fins during the ascent phase as they are covered by the main wings, reducing their effectiveness.

#### Technical Drawing

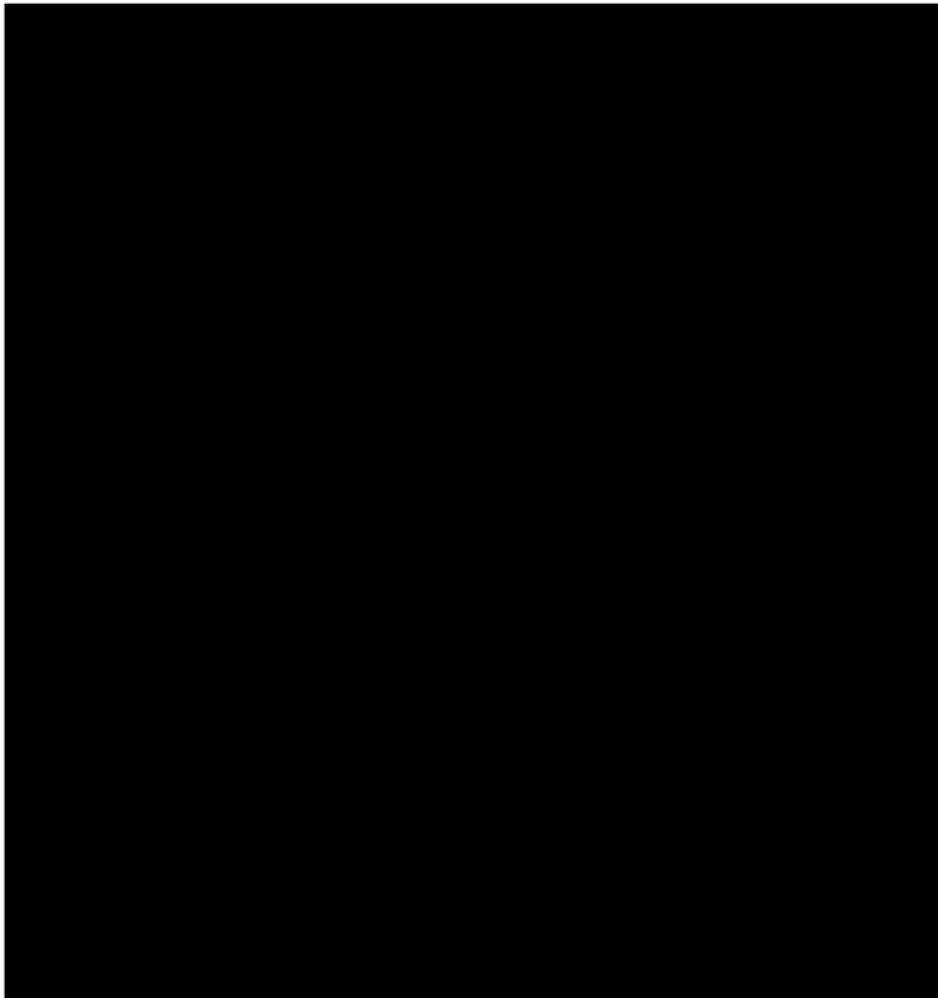


*Figure 6.1: Tail fins Technical Drawing*



### 6.3 Tail Fins Manufacture

The Tail Fins are 3D printed from PLA, with tri-hexagon infill pattern and an infill density [REDACTED] resulting in total mass of each fin being [REDACTED]

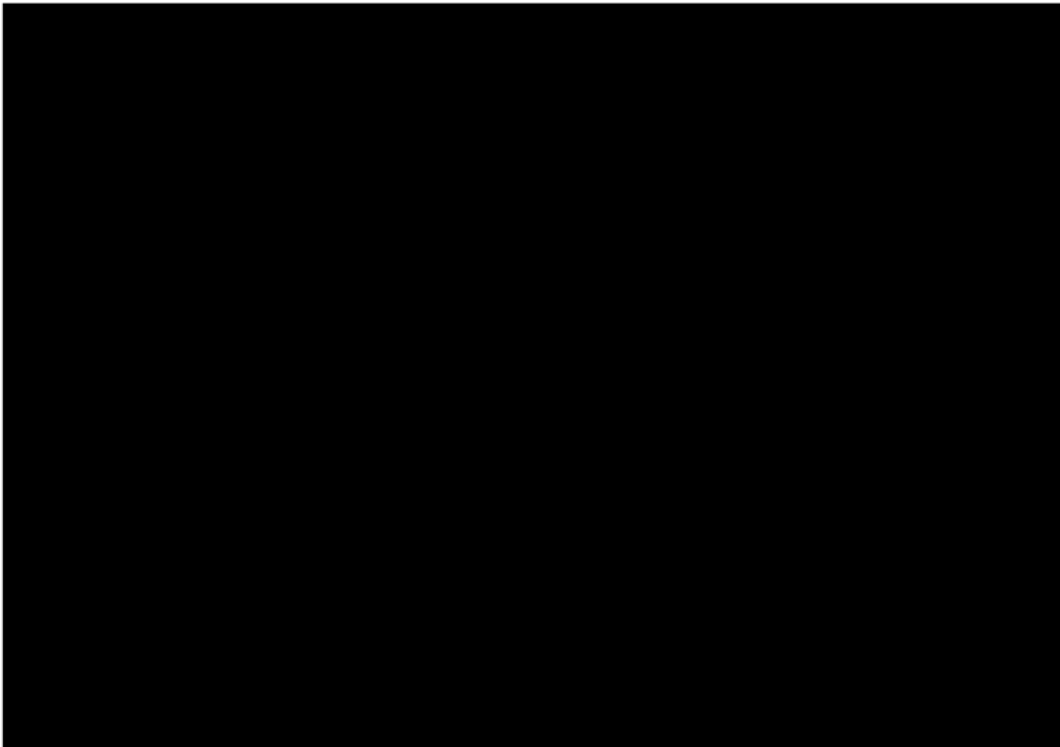


*Figure 6.2: Photo 1 of 3D Printed Tail Fin*

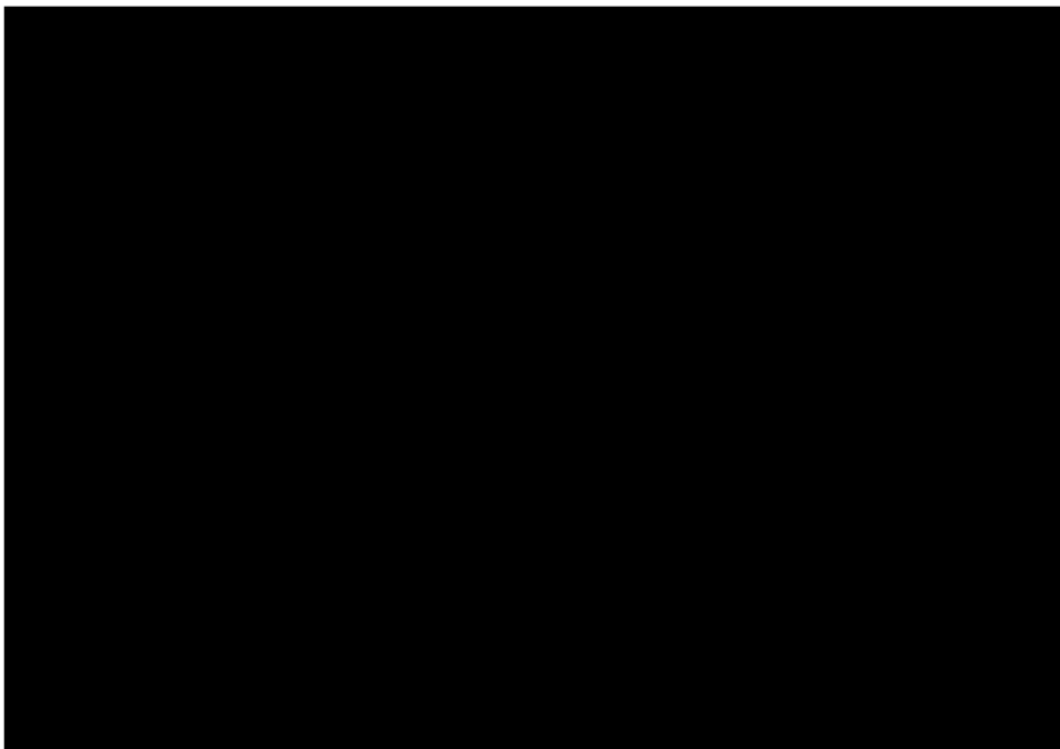


*Figure 6.3: Photo 2 of 3D Printed Tail Fin*

## 6.4 Main Wings

### Airfoil

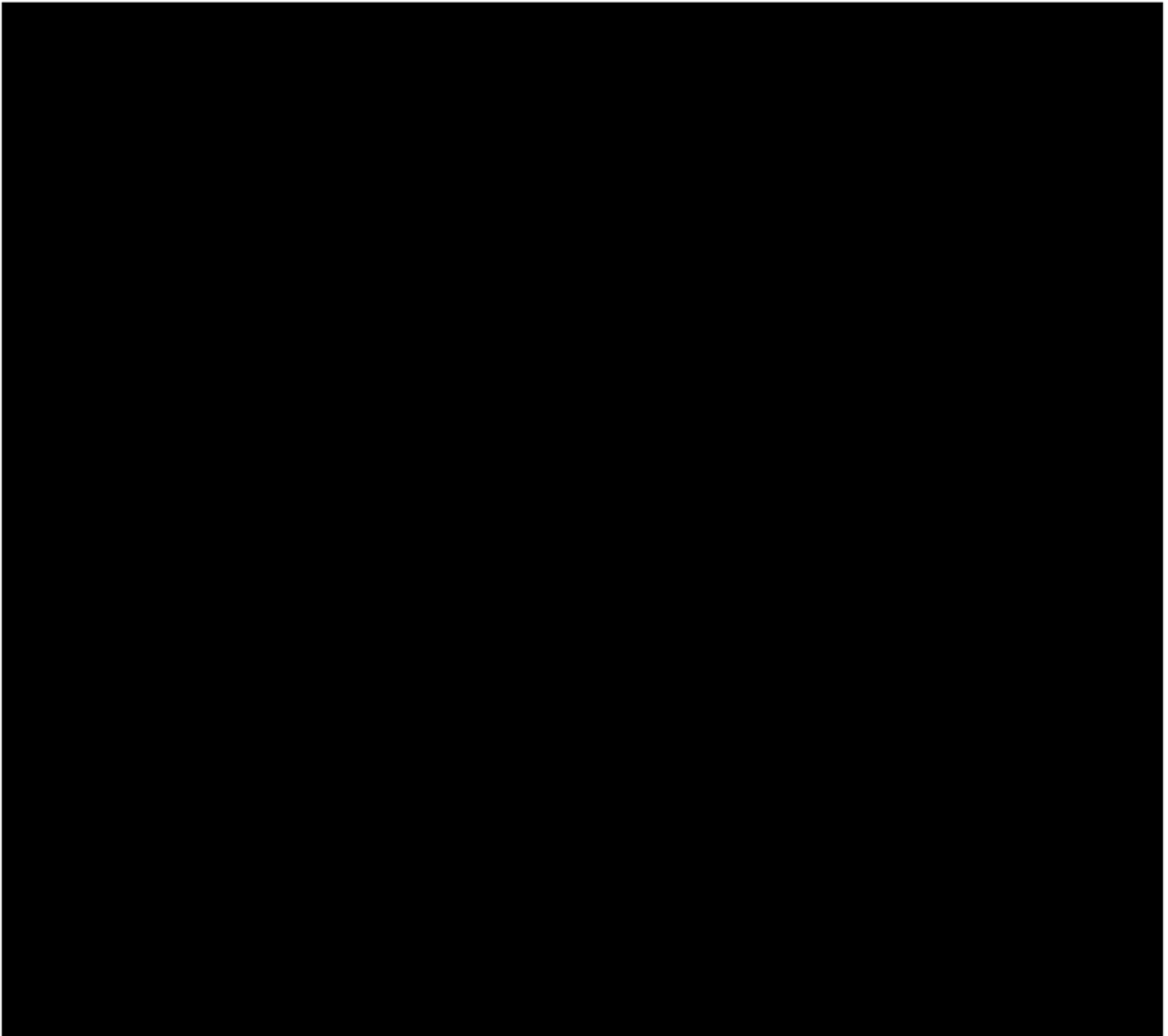
For the main wing attention was given to the selection of airfoil. Several high-lift, low-Raynolds number airfoils were considered such as:

- [REDACTED]
- [REDACTED]
- [REDACTED]
- [REDACTED]
- [REDACTED]
- [REDACTED]
- [REDACTED]
- [REDACTED]
- [REDACTED]
- [REDACTED]
- [REDACTED]
- [REDACTED]
- [REDACTED]

The airfoils were chosen based on the following data <sup>[6]</sup> [REDACTED]

- [REDACTED]
- [REDACTED]
- [REDACTED]
- [REDACTED]

Of the listed airfoils above, the ones selected were the [REDACTED] as the better performing ones. Their specifications are shown in the table of the next page.



Eventually due to manufacturing constraints, despite the favourable performance of [REDACTED] was chosen.

### Wing Design

The wing is designed to stall at the lowest possible speed, meaning that the wing area was directly affected. The chord length was maximized at [REDACTED] to provide enough authority for the horizontal stabilizers. The wing length was also maximized at [REDACTED], with the wing tip reaching the end of the nozzle. This resulted in a total wing area of [REDACTED].

### Technical Drawing

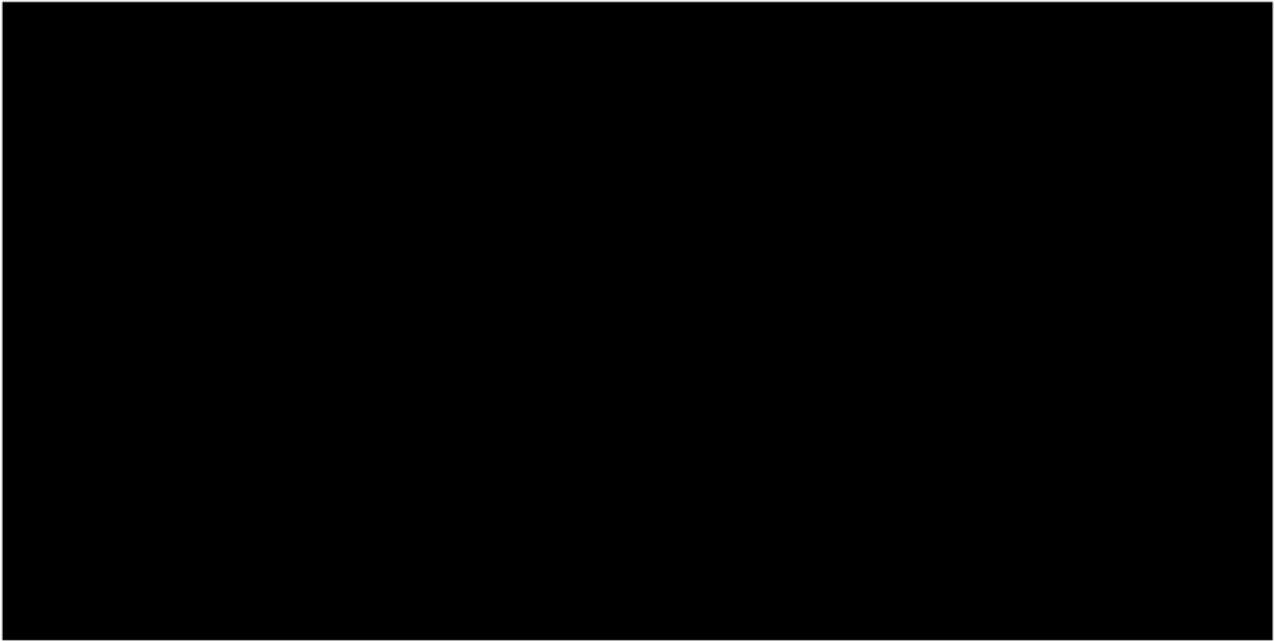


*Figure 6.4: Technical Drawing of Main Wing*

### Deployment Mechanism

The wings are attached to gears that mesh resulting in linked, simultaneous deployment of the wings. The deployment is triggered electronically via an Arduino type controller. A barometric sensor detects when the decent phase begins and immediately releases the release pin via the solenoid actuator. This frees the slider which is tensioned by the rubber band. The spring-loaded slider moves backwards pushing the rods in the extended position, deploying the wings. To achieve passive aerodynamic stability, the center of lift was moved rearwards by sweeping the wings at an angle of [REDACTED] degrees, when fully extended.

## 6.5 CFD Simulations

Simulations were conducted on the aircraft both in the wings deployed state and the wings stowed state to allow for drag and lift coefficient calculations to be used in the FDPS.

### Assumptions

- 1.
- 2.
- 3.
- 4.
- 5.



### Results

Velocity fields for wings stowed at different planes are shown in figures 6.5 and 6.6 below.

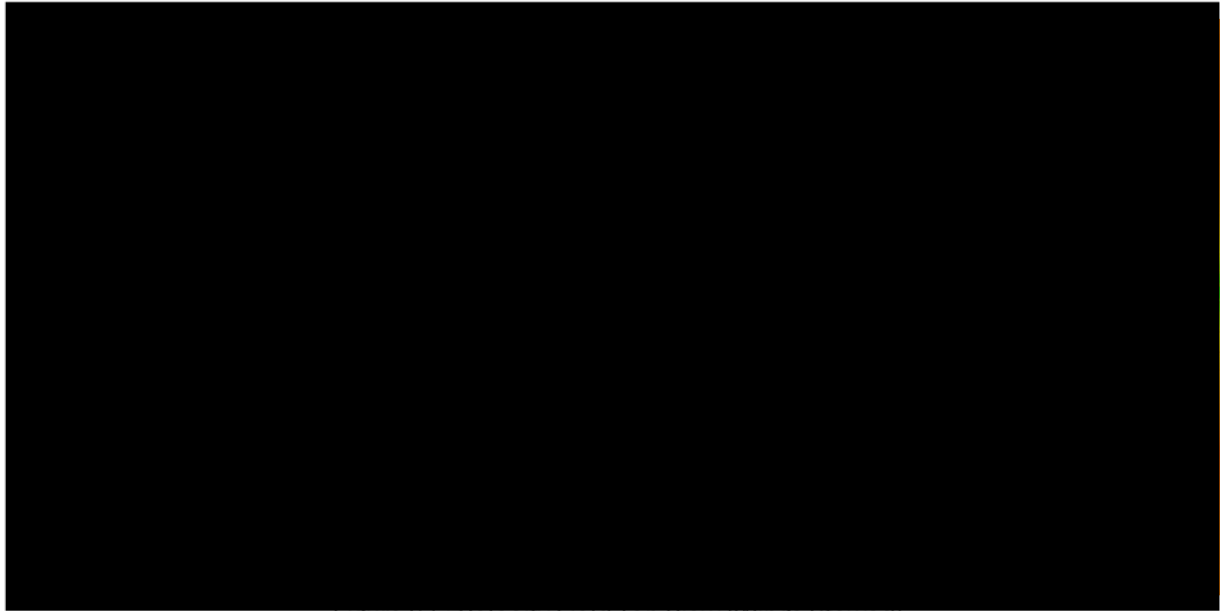


*Figure 6.5: Velocity Field Top View (Wings Stowed)*

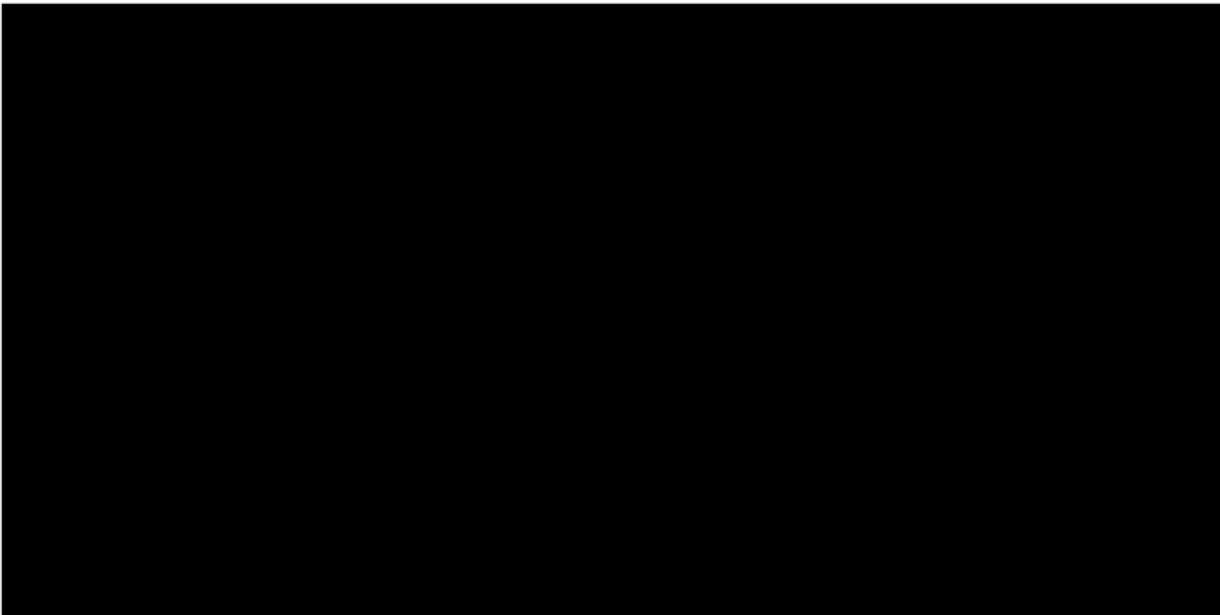


*Figure 6.6: Velocity Field Side View (Wings Stowed)*

Velocity fields for wings deployed at different planes are shown in figures 6.7 and 6.8, below.

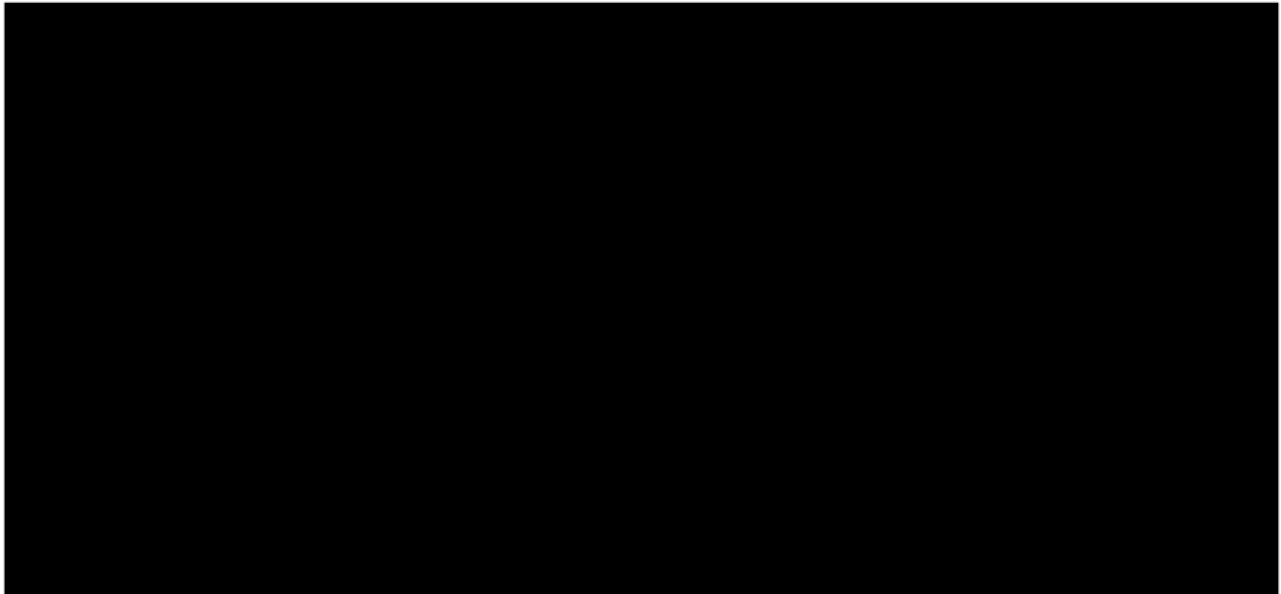


*Figure 6.7: Velocity Field Side View (Wings Deployed)*

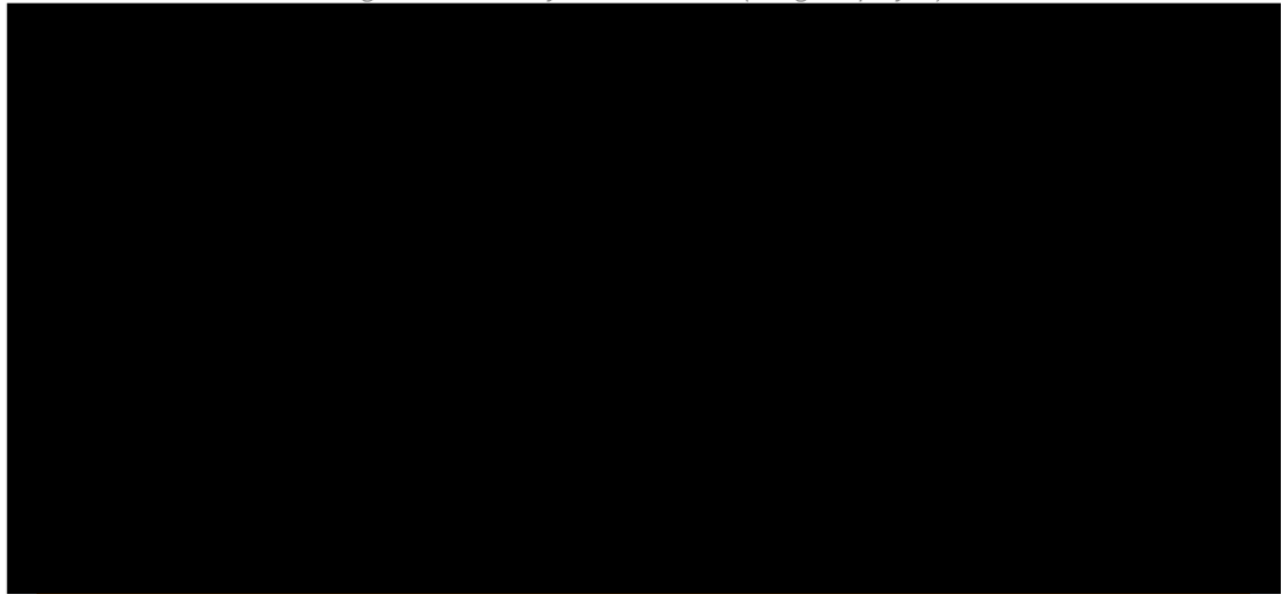


*Figure 6.8: Velocity Field Top View (Wings Deployed)*

From the simulations a negative (nose down) pitching moment [REDACTED] was identified confirming the passive aerodynamic stability of the aircraft.

The simulation resulted in the following drag coefficient values:

Drag Coefficient Values	
[REDACTED]	[REDACTED]
[REDACTED]	[REDACTED]

*Table 6.1: Drag Coefficients*

## 6.6 Wing Manufacturing

High durability foam was selected for the main wings, that is reinforced with wooden sticks. The wings are shaped in a custom-made foam-cutter using guide rails (*Figure 6.9*) in the shape of the airfoil. The surface of the wings is coated with a thin tape to allow for lower skin friction.



*Figure 6.9: Foam Cutting Guide Rails*

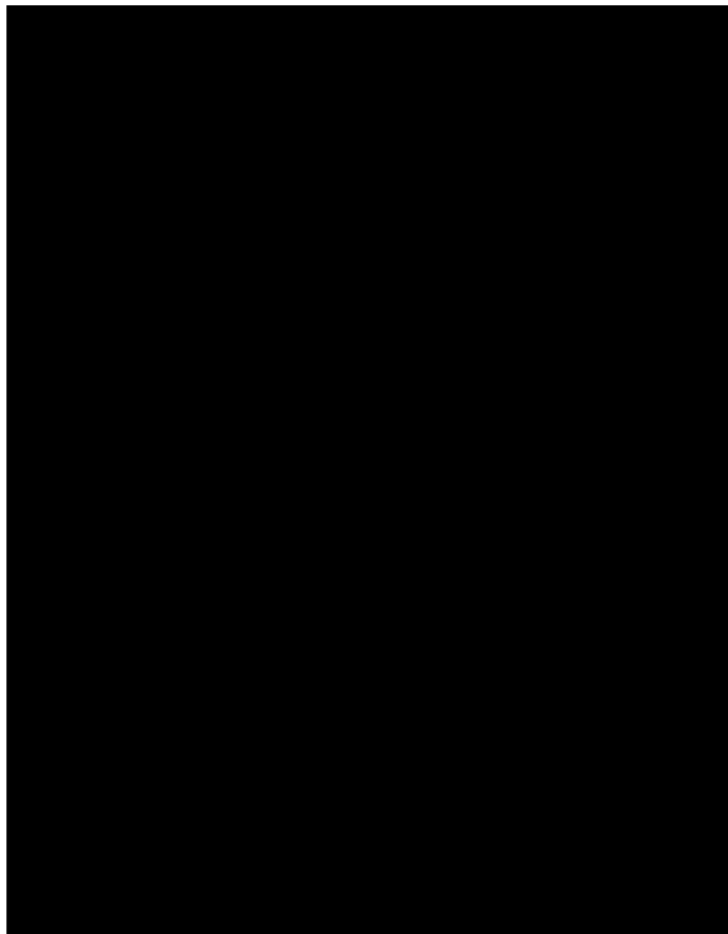


*Figure 6.10: Finished Wings*

## 7. Simulators - Flight Modelling

The aircraft performance was modeled using two separate simulators that were specifically designed for this project. Through their data outputs the team was able to determine the impact of all possible inputs on flight performance, and eventually the final score.

### 7.1 FDPS

The **Flight Dynamics and Performance Simulator (FDPS)** gets environmental parameters and initial launch motion data which are calculated externally (The initial launch motion data are obtained through a web-based water rocket simulator<sup>[1]</sup>), to calculate the following flight-time dependent variables:

- Range
- Altitude
- Vertical Speed
- Lateral Speed
- Acceleration
- Drag
- Lift

The FDPS data inputs including lift and drag coefficients, wing area and mass where initially rough estimates, that were adjusted over a wide range of consecutive iterations in order to approach meaningful and realistic outputs. Finally, performance with or without foldable wings can be opted to be calculated allowing for easy comparisons between the two modes.

#### Assumptions

##### Flight Dynamics Analysis

1. The aircraft is considered a point mass.
2. Deployment of wings is considered instantaneous.
3. Gliding angle of attack is considered constant.

##### Propulsion Analysis

1. Fluid flow within the propulsion tank is considered laminar and unidirectional.
2. Volume for the pressurized propulsion tank is considered 3% greater than that of the unpressurized tank.
3. The tank is considered fully sealed meaning that no propulsion fluid escapes until clear of the launch tube.

The above assumptions are made in the flight model, in addition to the environmental assumptions discussed in *Propulsion Analysis (Section 5.2)*.



## Inputs

As previously discussed, the burnout data were externally calculated with the following inputs:

Rocket	
Rocket Outside Diameter (mm)	
Nozzle Exit Diameter (mm)	
Total Volume (L)	
Water Amount (L)	
Empty Mass (g)	
Drag Coefficient	
Nozzle Adjuster A	
Nozzle Adjuster B	
Nozzle Adjuster C	
Water Thrust Efficiency	
Gas Thrust Efficiency	
Launcher	
Pressure (bar)	
Launch Tube Diameter (mm)	
Launch Tube Length (mm)	
Launcher Volume (L)	
Gas Source	
Liquid Density (g/cm^3)	
Environment	
Ambient Temperature (C)	
Ambient Pressure (Pa)	
Relative Humidity in Rocket %	
Gravity (m/s^2)	

Figure 7.1: Inputs in external burnout data calculator

Resulting in the following burnout data:

Burnout Data	

Table 7.1: Burnout Data

The simulator input parameters are shown in the following table:

### Deployable Wings Advantage

In the figures below the impact of the deployable wings can be seen as an increase in range (and subsequently flight time) resulting in a greater score.



*Figure 7.2: Flight Profile graph without deployable wings system*

*FIGURE 7.3: FLIGHT PROFILE GRAPH WITH DEPLOYABLE WINGS SYSTEM*

### Outputs

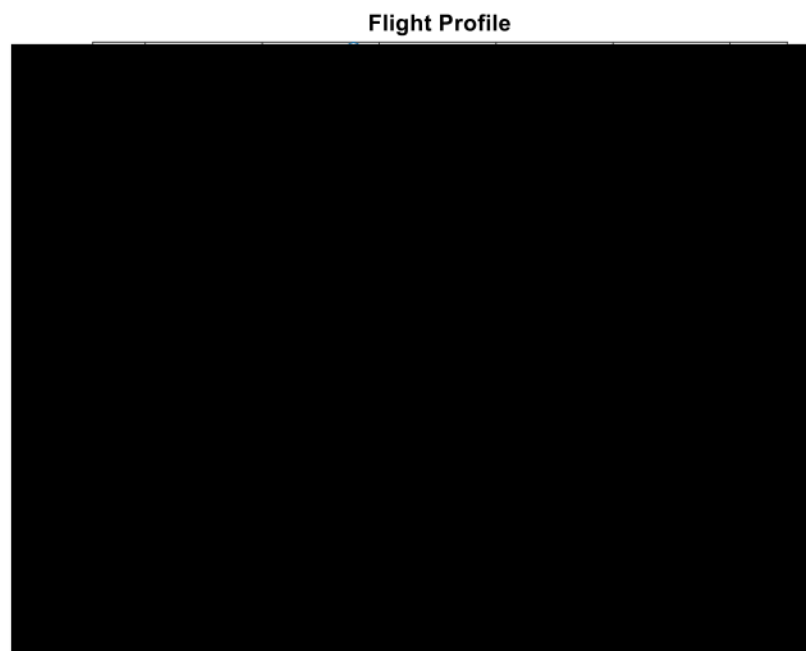


*FIGURE 7.4: FLIGHT PROFILE GRAPH*

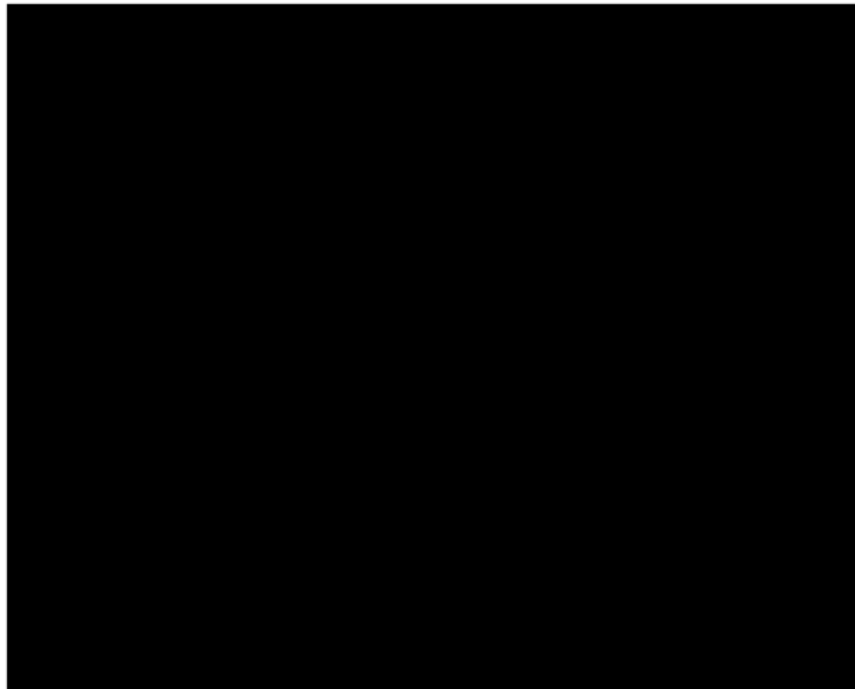


*Figure 7.5: Altitude – Range graph*

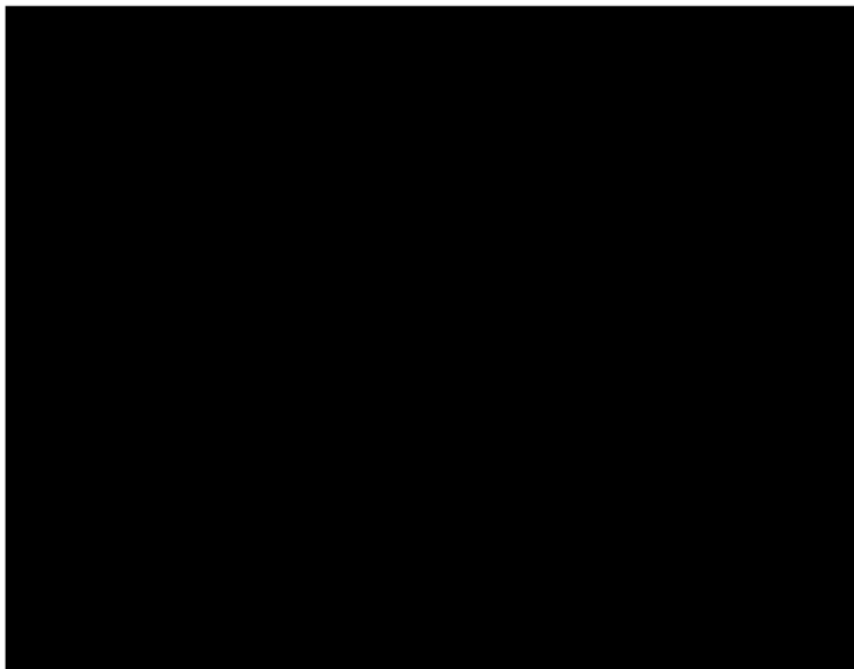


*Figure 7.6: Vertical – Lateral Speed graph*

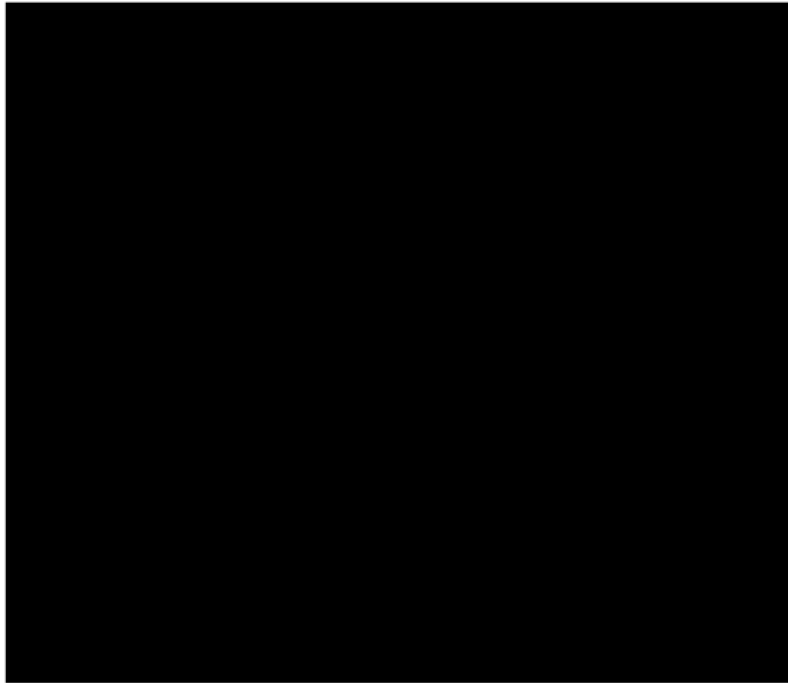


*Figure 7.7: Pitch angle – Time graph*

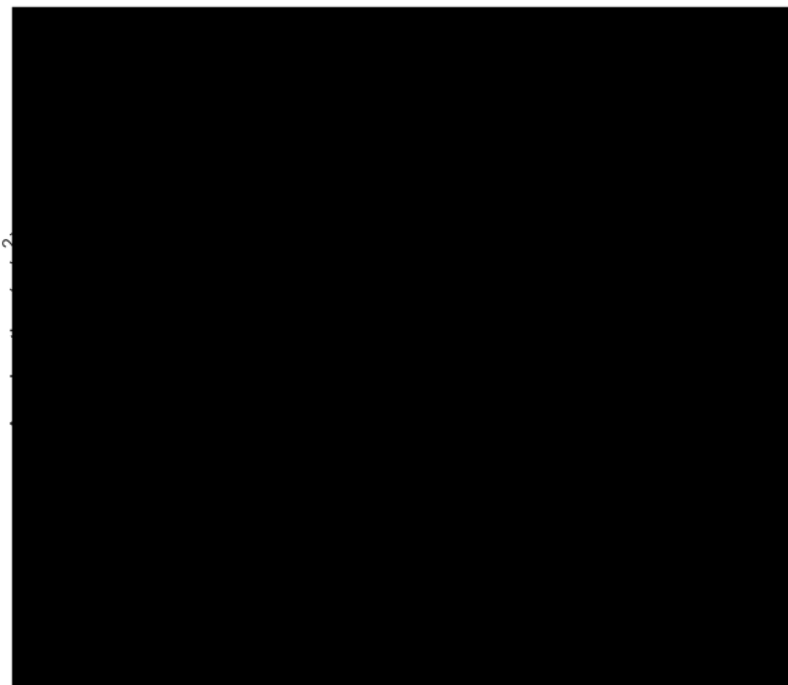


*Figure 7.8: Horizontal – Vertical Acceleration graph*

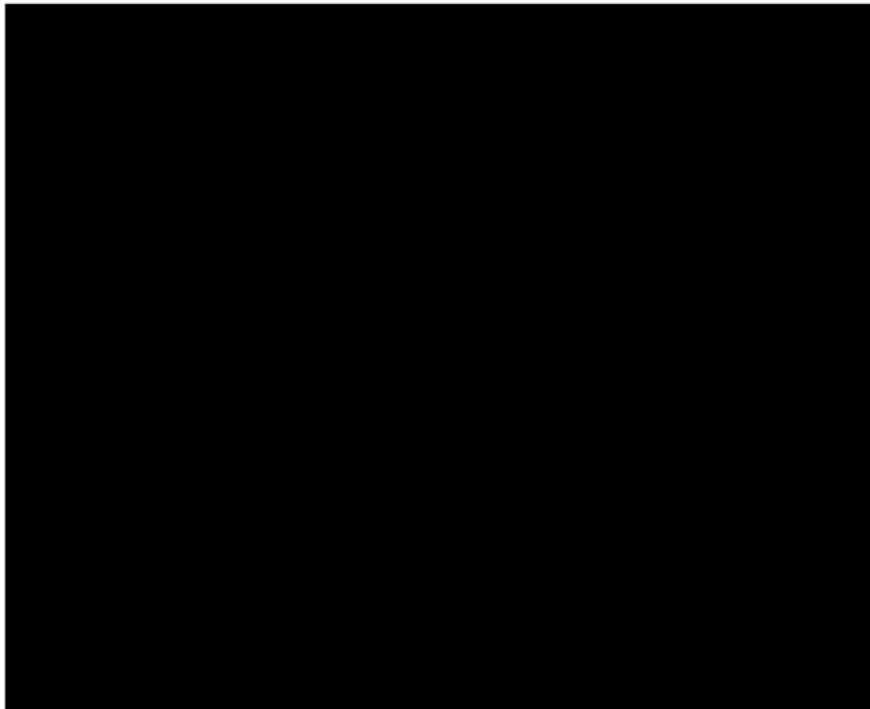


*Figure 7.9: Drag – Lift Graph*

The following table shows the estimated score data.

Score Data

*Table 7.2: Score Data*

## 8. Sloshing Management – Tank Design

### General

The payload tank as determined in Section 3.2 needs to carry 0.75kg of water, so the tank was designed with a volume of 1.5L to allow for 50% fill level. The tank is located in the forward part of the aircraft to induce passive aerodynamic stability.

### Damping Mechanism

In order to address the sloshing of the water inside the payload tank a passive control system was selected. Passive control is achieved through a single flexible baffle.

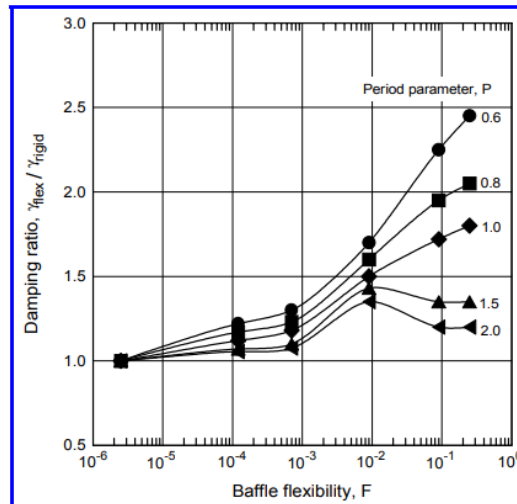


Figure 8.1: Damping as a function of flexibility  $F$  [STEPHENS & SCHOLL, 1967]

The baffle was designed to comply with the 50% cross-sectional area rule and was placed in the middle of the payload tank. A flexible material (insert material) was selected to improve the damping of the baffle. Flexible baffles' damping is better than damping from rigid baffles, thanks to the deformation absorbing large part of the kinetic energy of the sloshing liquid. As the baffle becomes more flexible, the relative damping increases (Figure 8.1). Consequently, flexible baffles can allow a substantial improvement in baffle damping efficiency <sup>[7]</sup>.

Perforating the baffle was also considered. Despite the benefit of oscillating flow through the holes acting as an additional source of damping, the baffle area is reduced and thus little is to be gained <sup>[7]</sup> in terms of damping.

Tank Design

The tank was a simple cylindrical shape made to both accommodate the baffle and provide enough volume to capacitate 0.75Liters of water with 50% filling capacity.

The table below shows the different parts in the tank.

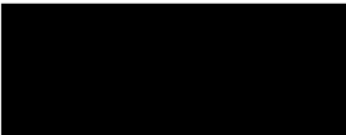
A rectangular area that has been completely blacked out, redacting the content of the table.

Table 8.1: Tank Parts

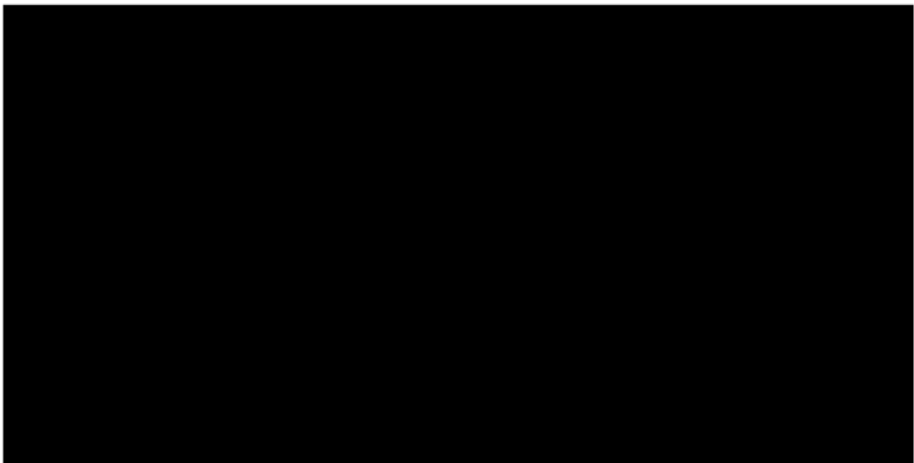


Figure 8.2: Tank Breakout View

Manufacturing

The baffle was 3D printed from a flexible filament, with a thickness of 2mm, and designed to fit inside the tank.

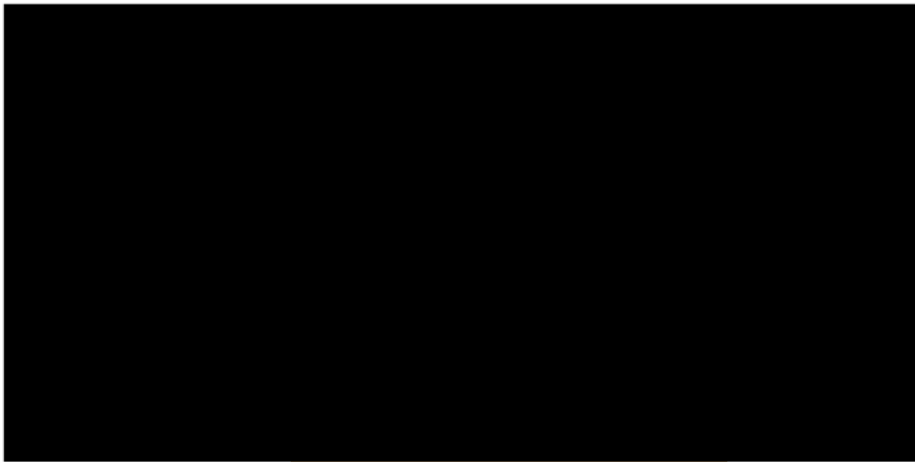
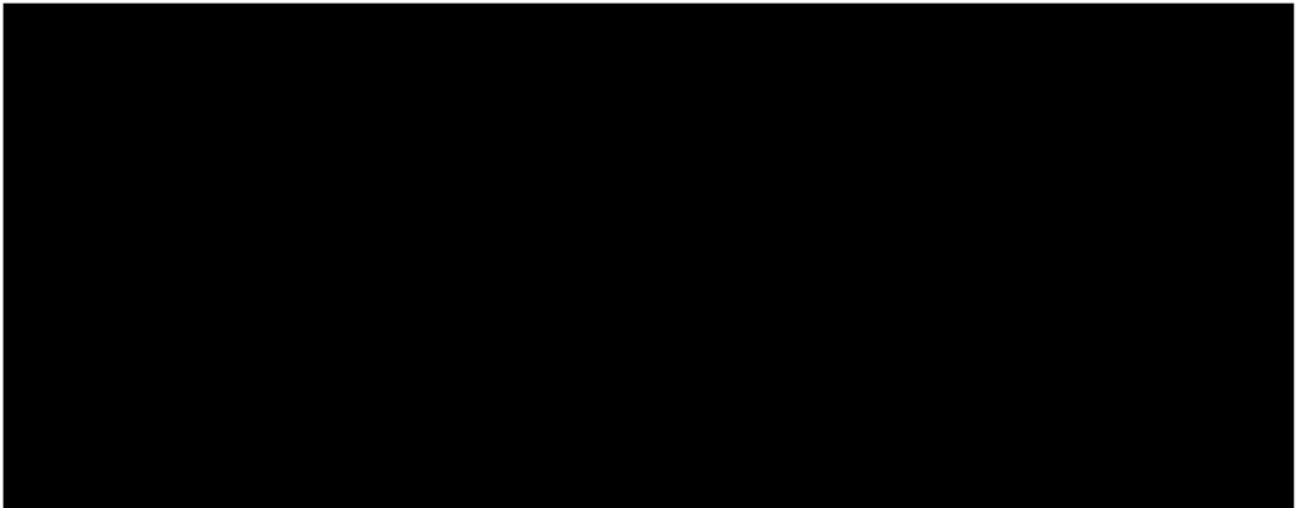


Figure 8.3: 3D Printed Flexible Baffle

## Simulation

The sloshing motion of the water was predicted using the OpenFOAM software that simulated the motion of the aircraft through FDPS data.



*Figure 8.4: Fluid motion without baffle at 1.35s*

*Figure 8.4*

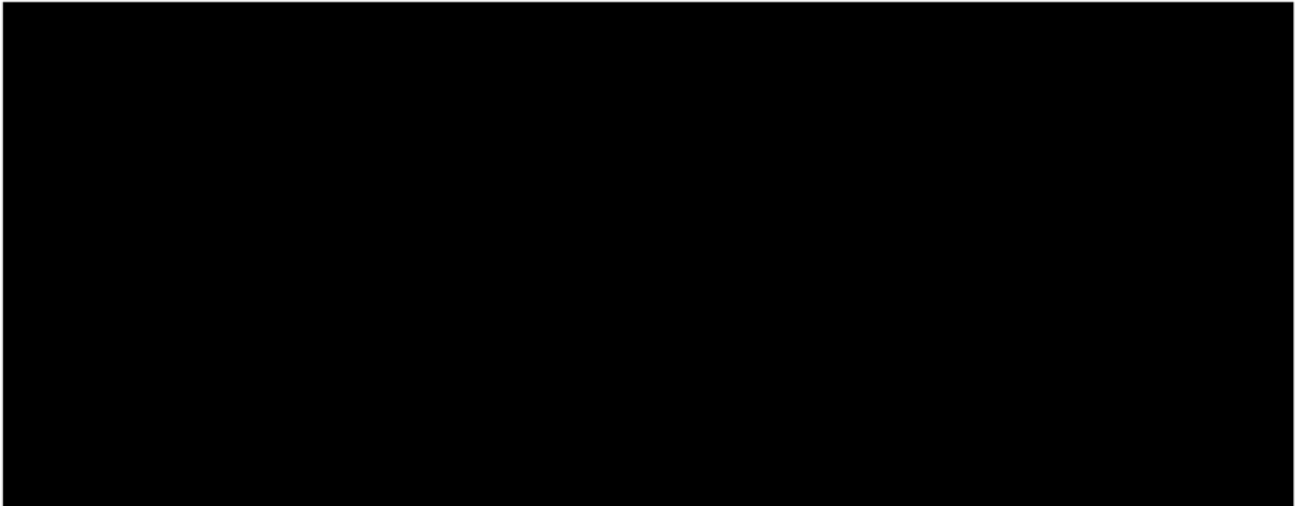


*Figure 8.5: Fluid motion without baffle at 1.5s*

As shown in the figures sloshing without the damping of baffles under the extreme forces during flight, results in a chaotic fluid flow, that negatively affects the overall stability of the rocket.



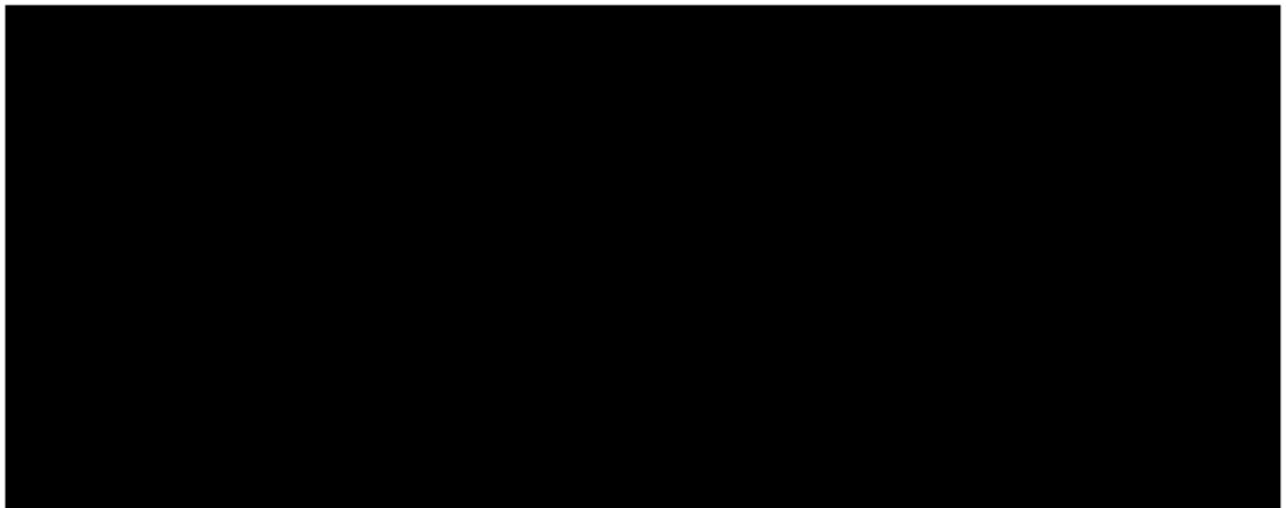


*Figure 8.6: Fluid motion with baffle at 1.35s*

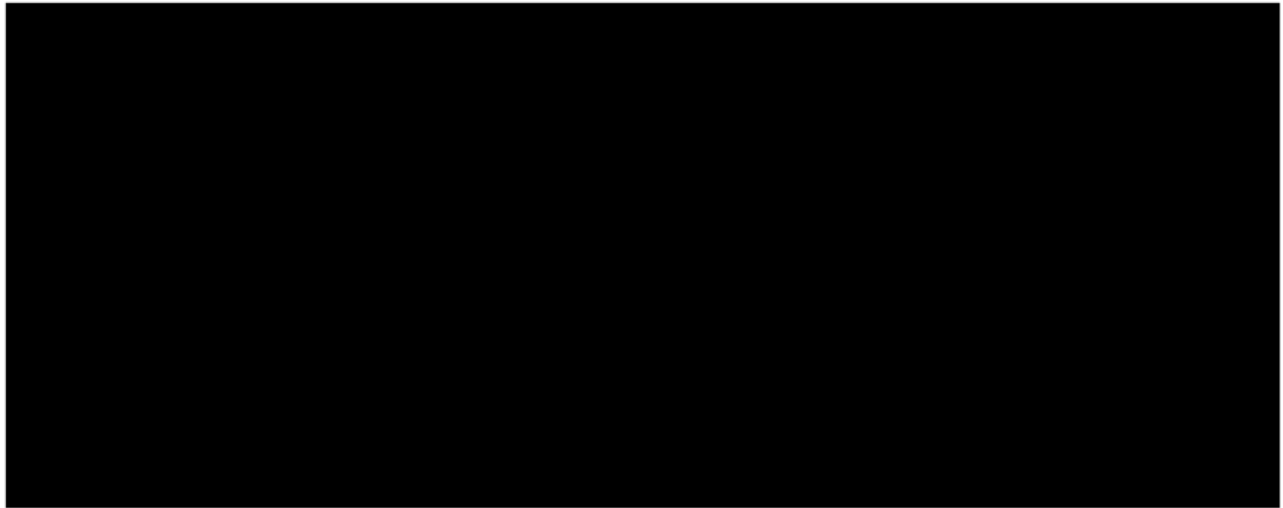
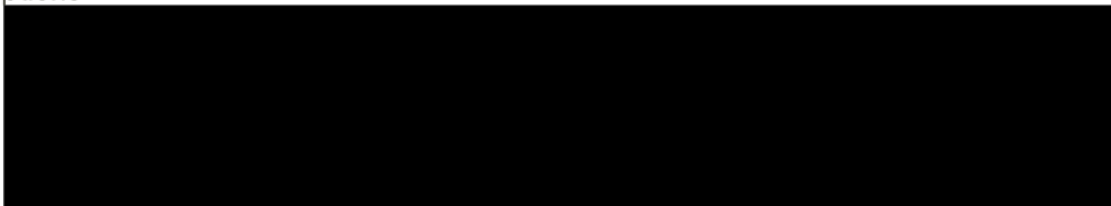


*Figure 8.7: Fluid motion with baffle at 1.5s*

Simulations with baffles allow for adequate damping of sloshing resulting in much more stable fluid motion and predictable movement of the center of gravity within the tank.

#### Assumptions

- 1.
- 2.
- 3.
- 4.



## 9. Structural Design

### 9.1 Materials

The design needs to be durable to be able to withstand the forces exerted during launch and at landing, while being as light as possible. To achieve this several materials were considered, including:

- 
- 
- 
- 
- 
- 
- 
- 



### 9.2 Main Load Bearing Structure

The main load bearing structure is made from long **oak wood** rods that were chosen over **balsa wood** for their increased durability and greater modulus of elasticity.

#### FEA

To test the integrity of the load bearing structure a finite element analysis was performed on the wooden rods. The loads were estimated via the FDPS data.

#### Load calculation

From FDPS data the velocity of impact is calculated at  $v =$  [redacted]. Assuming an impact duration [redacted] the load exerted on the rods is:

$$F = \frac{\Delta p}{\Delta t}$$
$$F = m \cdot \frac{\Delta v}{\Delta t} =$$
 [redacted]

The material assumed for the simulation was MDF (Medium Density Fiberboard) as typical wood is anisotropic and cannot be simulated with finite methods. MDF provides conservative results, since it is less durable than typical oak wood. The specifics of the MDF are shown in the table below.

Density	[redacted]
Young's Modulus	
Poisson's Ratio	
Yield Strength	
Ultimate Tensile Strength	

Table 9.1: Material Specifications

Force Data	[redacted]
Magnitude	
X Angle (offset from rod axis)	

Table 9.2: Applied Force Details

## Results

The simulation resulted in small elastic displacements and was completed successfully verifying the structural integrity of the rods.

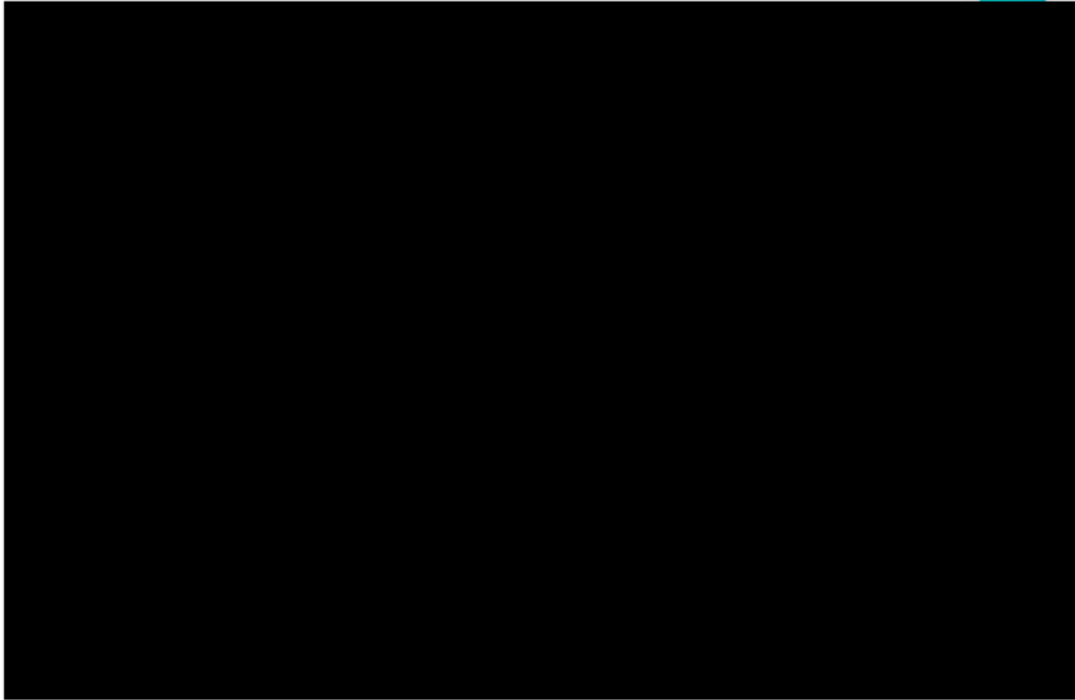


*Figure 9.1: FEA Results (Displacement)*

### 9.3 Nose Cone

The nose cone is constructed from [REDACTED] excellent shock absorption characteristics and its low density.

### 9.4 Main Wings

The main wings are made from [REDACTED], to ensure flexibility and durability. The propulsion tank is a soda bottle. The bottle is made from PET which makes it durable under high pressure loads.

### 9.5 Propulsion Tank

A typical PET bottle of a volume of 1.5L was selected based on the PTES simulation results.

## 9.6 3D-Printed parts

All other parts of the aircraft were made with 3D printable materials of whom [REDACTED] was selected for its high ultimate yield strength and low density. Additionally, during manufacturing infill densities and patterns were adjusted to achieve a balance between durability and mass.

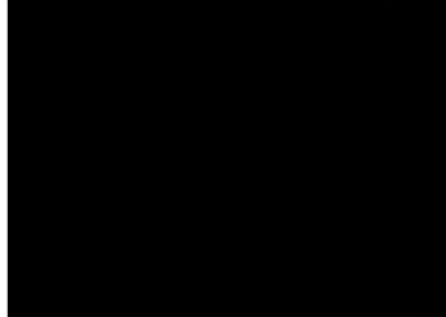
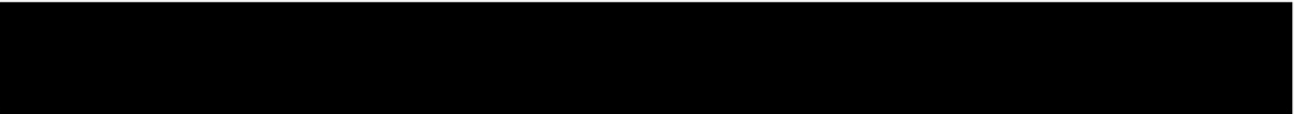


Figure 9.2: Tri-hexagon pattern<sup>[8]</sup>



## 10. Control

Control of the aircraft during flight is crucial as it allows for adaptability and performance flexibility. The aircraft is radio-controlled with the aim of achieving full autonomy in the future. To simplify construction and lower weight, only pitch and yaw control are available. Thus, roll stability is achieved passively through the wings' aerodynamic design.

The DX6i radio-controlled module was used alongside the SG-90 9G servo motors which were linked to the control surfaces through thin steel wire links.



Figure 10.1: Radio Control Module

## 11. Bill of Materials

[illegible]

Table 12.1: Bill of Materials

First Prototype

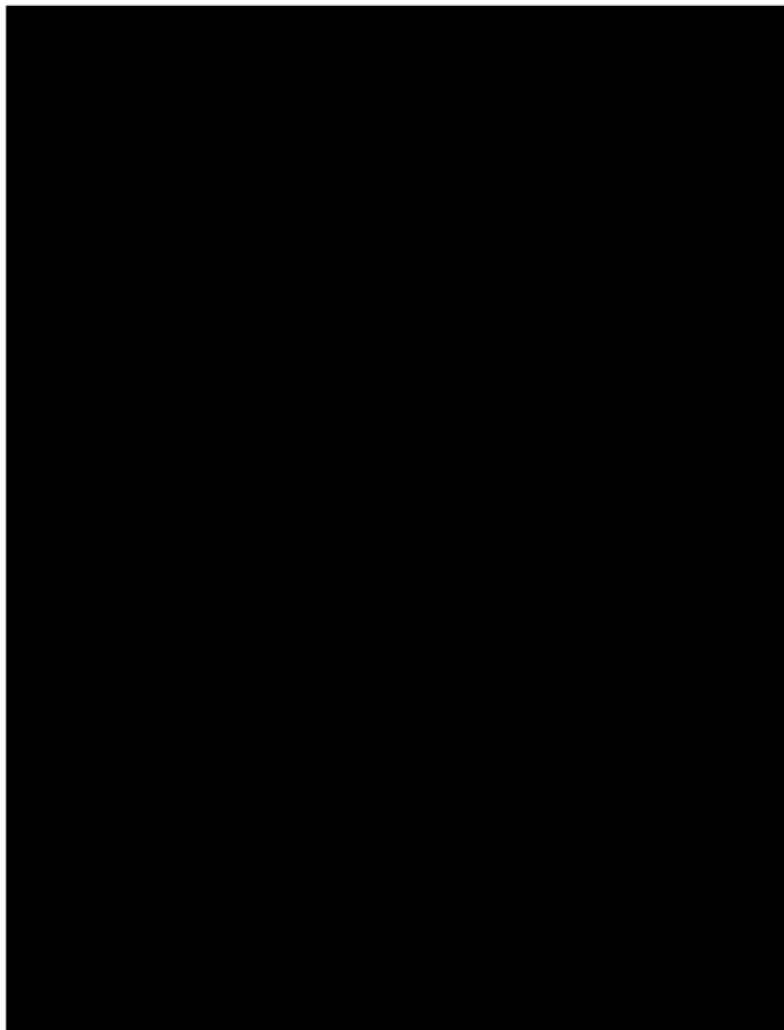


*Figure 11.1: Prototype*

## 12. Risk Assessment

The report below, sums up the hazards identified and the risk lever for each one.

Likelihood	5 - Very Likely					
	4 - Likely					
	3 - Possible					
	2 - Unlikely					
	1 - Extremely Unlikely					
	Risk Matrix		1- Minor Injury / No First Aid required	2 - Minor Injury / First Aid Required	3 - Injury / requires treatment or Hospital attendance	4 - Major Injury
		Severity				

Table 12.1: Risk Matrix

POINTS:	RISK LEVEL:	ACTION:
1 – 2	NEGLIGIBLE	No further action is necessary.
3 – 5	TOLERABLE	Where possible, reduce the risk further
6 - 12	MODERATE	Additional control measures are required
15 – 16	HIGH	Immediate action is necessary
20 - 25	INTOLERABLE	Stop the activity/ do not start the activity

Table 12.2: Risk Levels

Identified Hazards	Likelihood Level	Severity Level	Risk Lever ( Severity x Likelihood)

Table 12.3: Identified Hazards and related risks

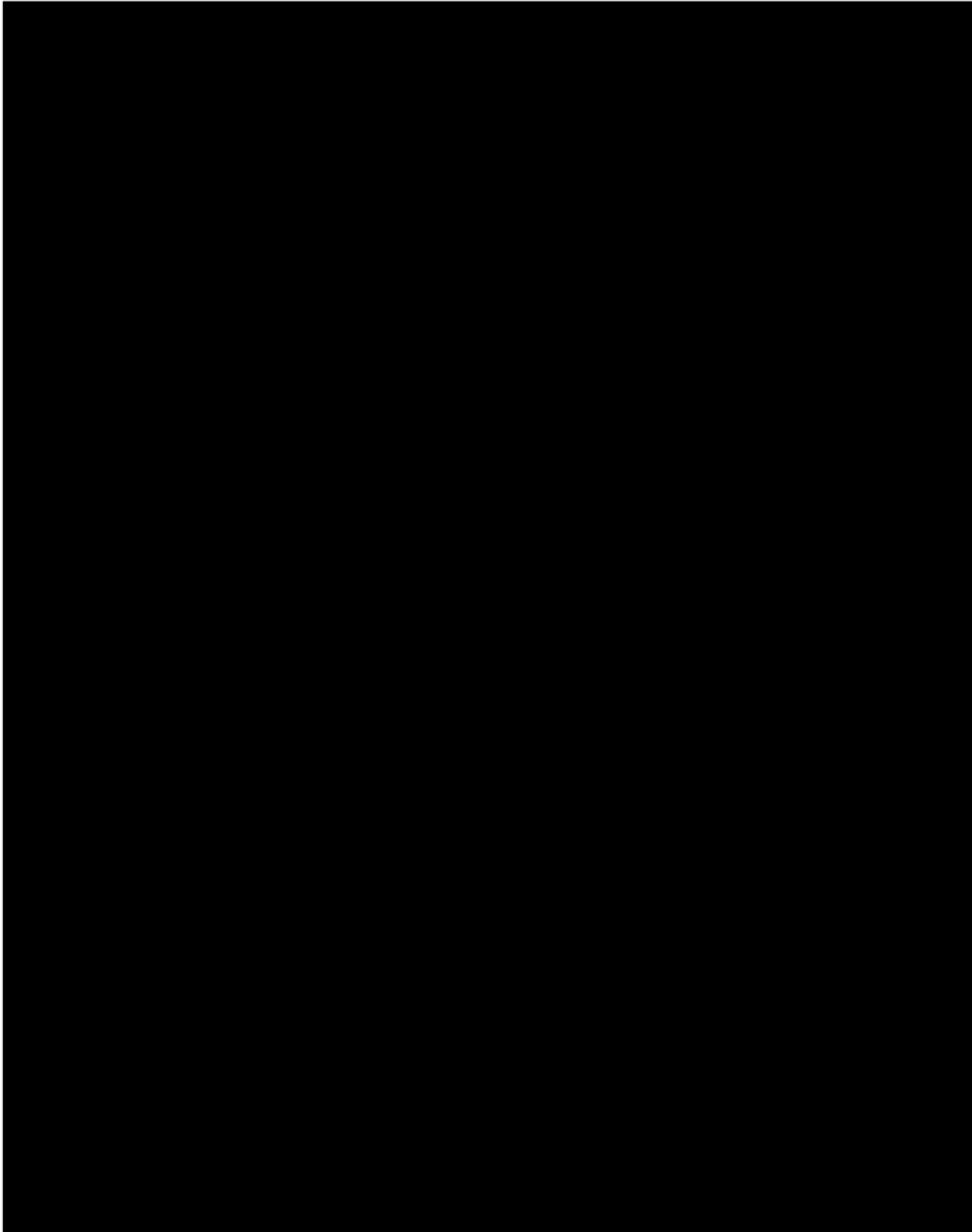
## Conclusion

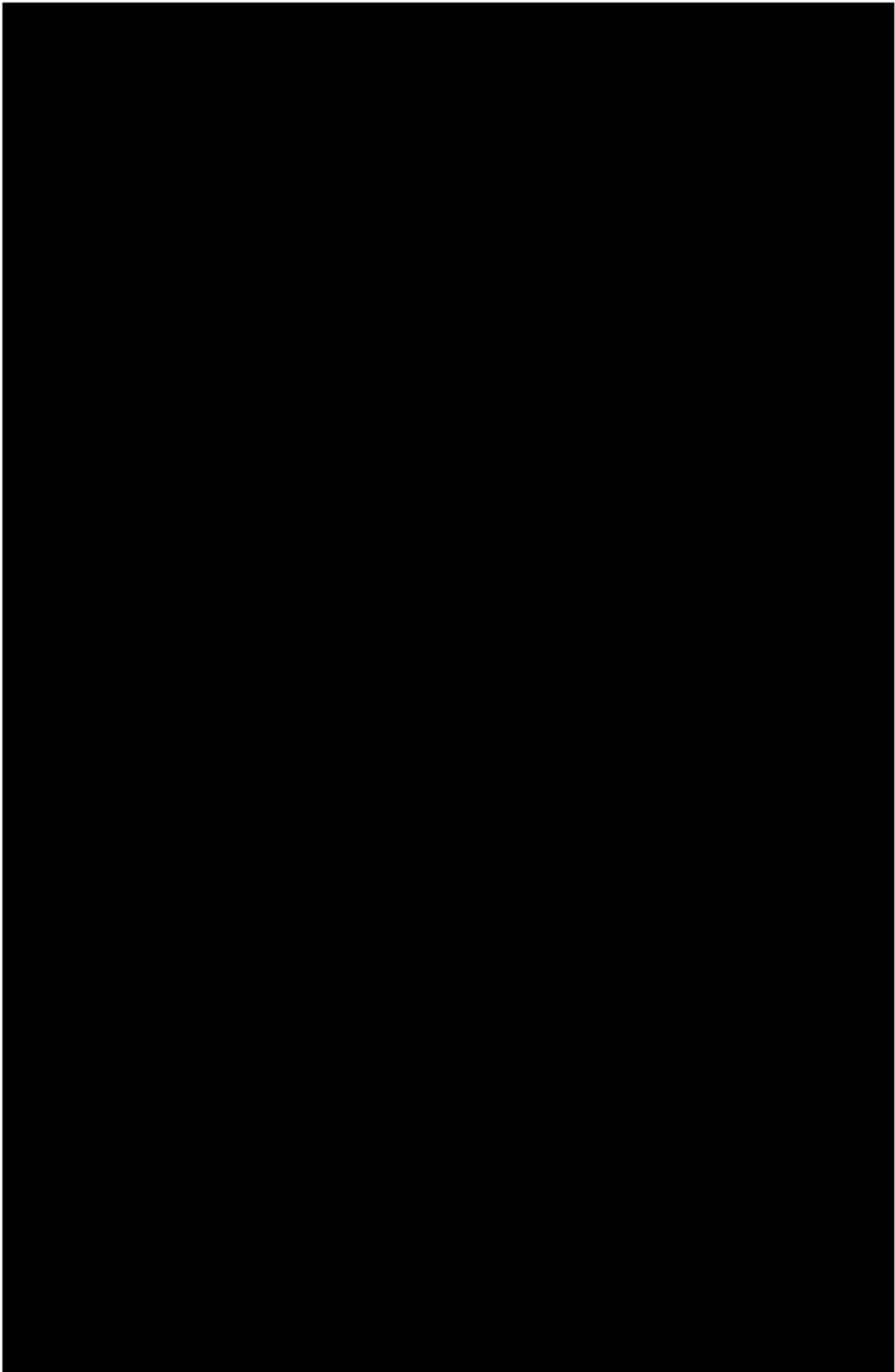
In the future the aircraft will be subjected to flight tests for validation and calibration of the models used. This report includes all the design choices made in this short time frame (January – May). Some choices may prove to be wrong through testing, so inevitably design changes will come with the aim of achieving better performance.

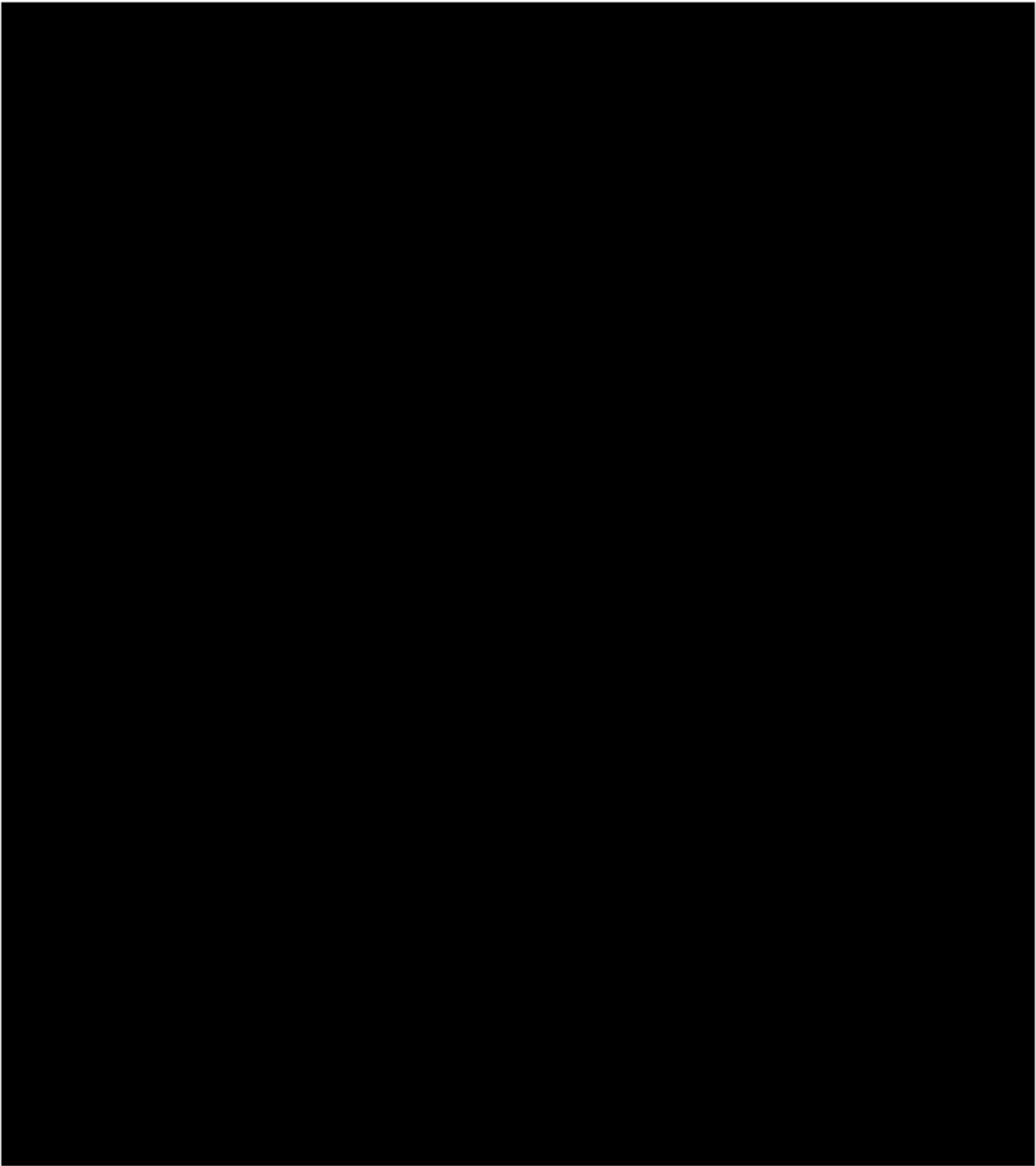


## Appendix

### FDPS Matlab Code



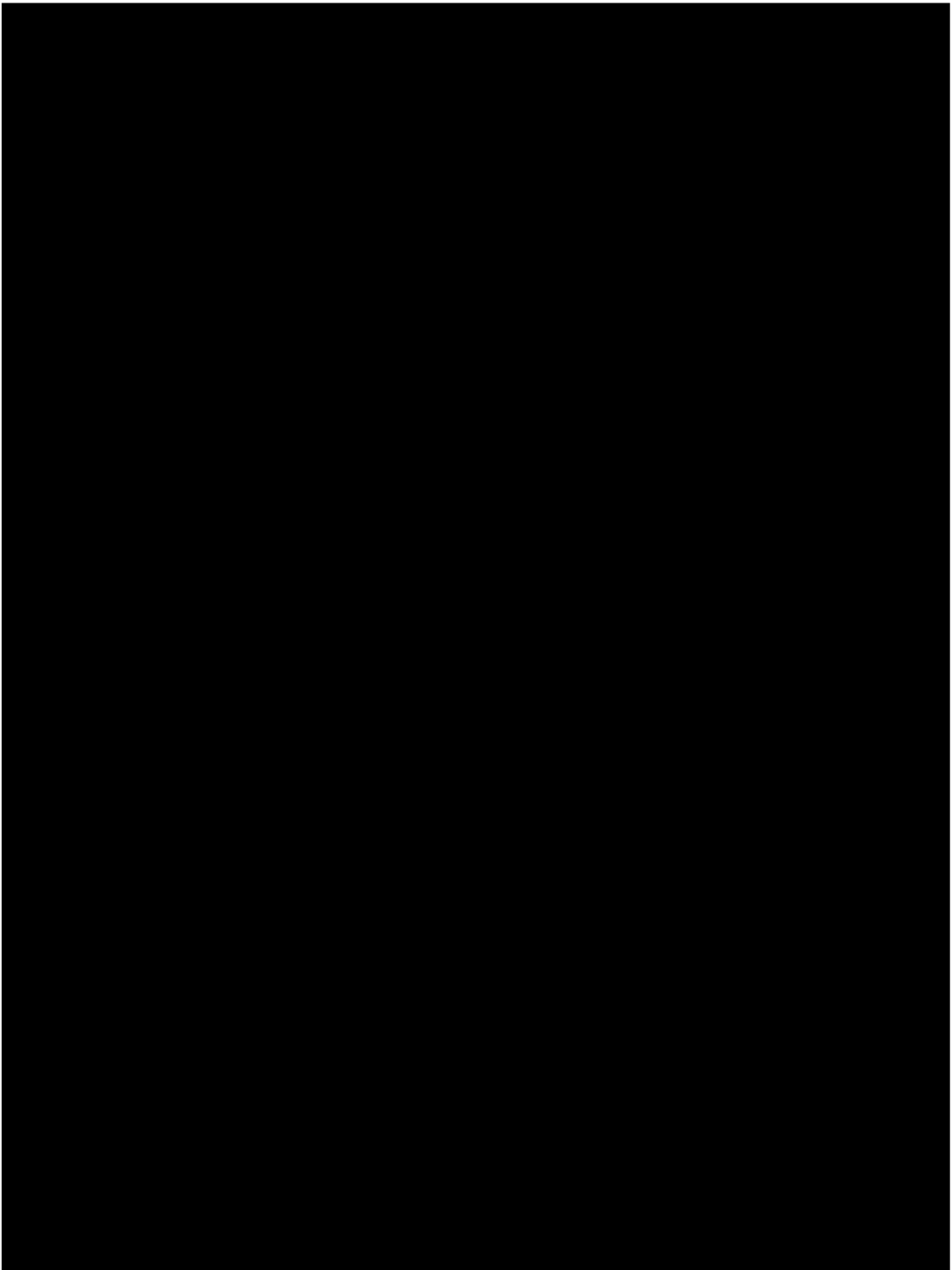


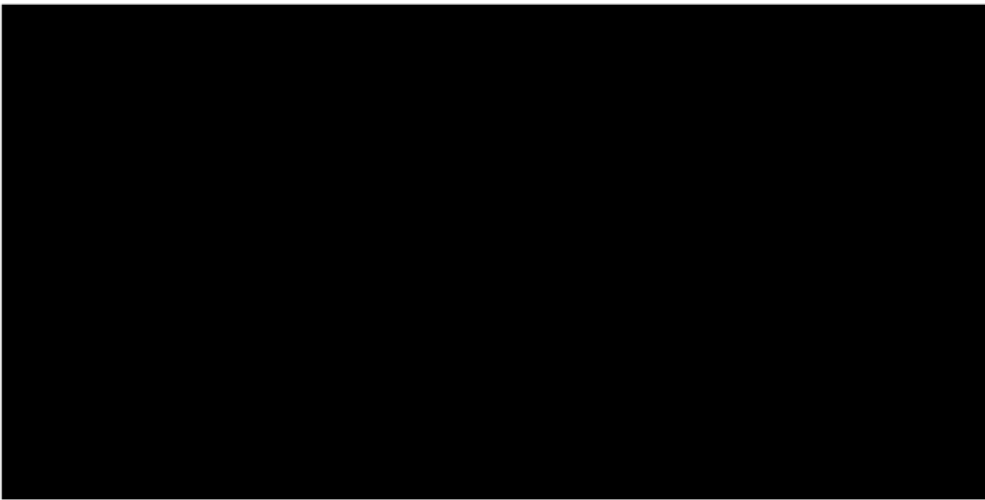


## PTES Matlab Code

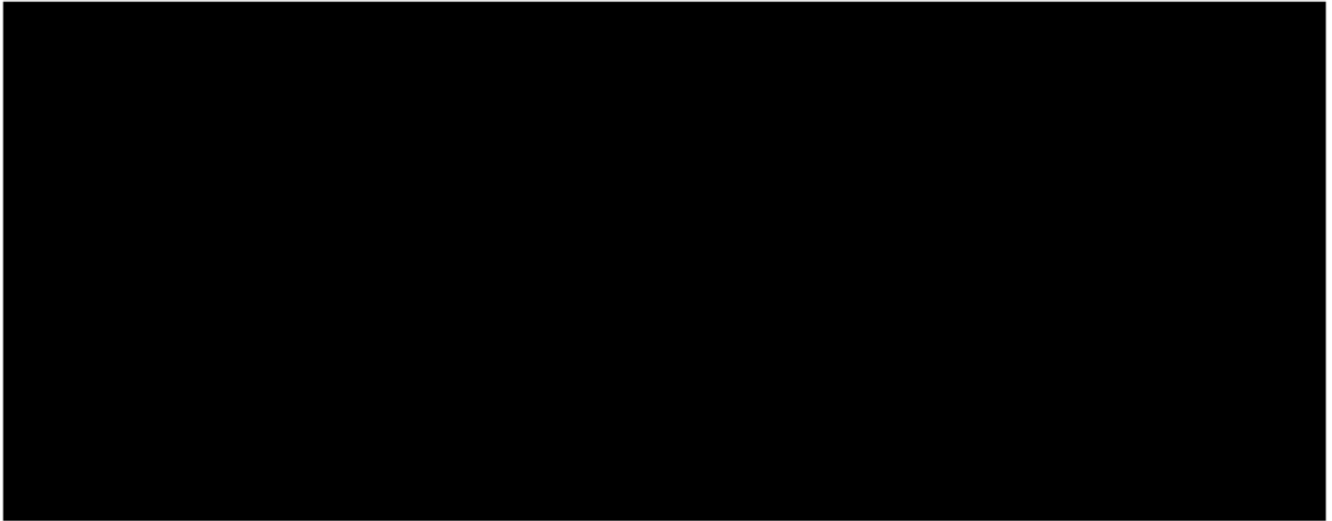
%Propulsion - Thrust Efficiency Simulator

%% Main Script

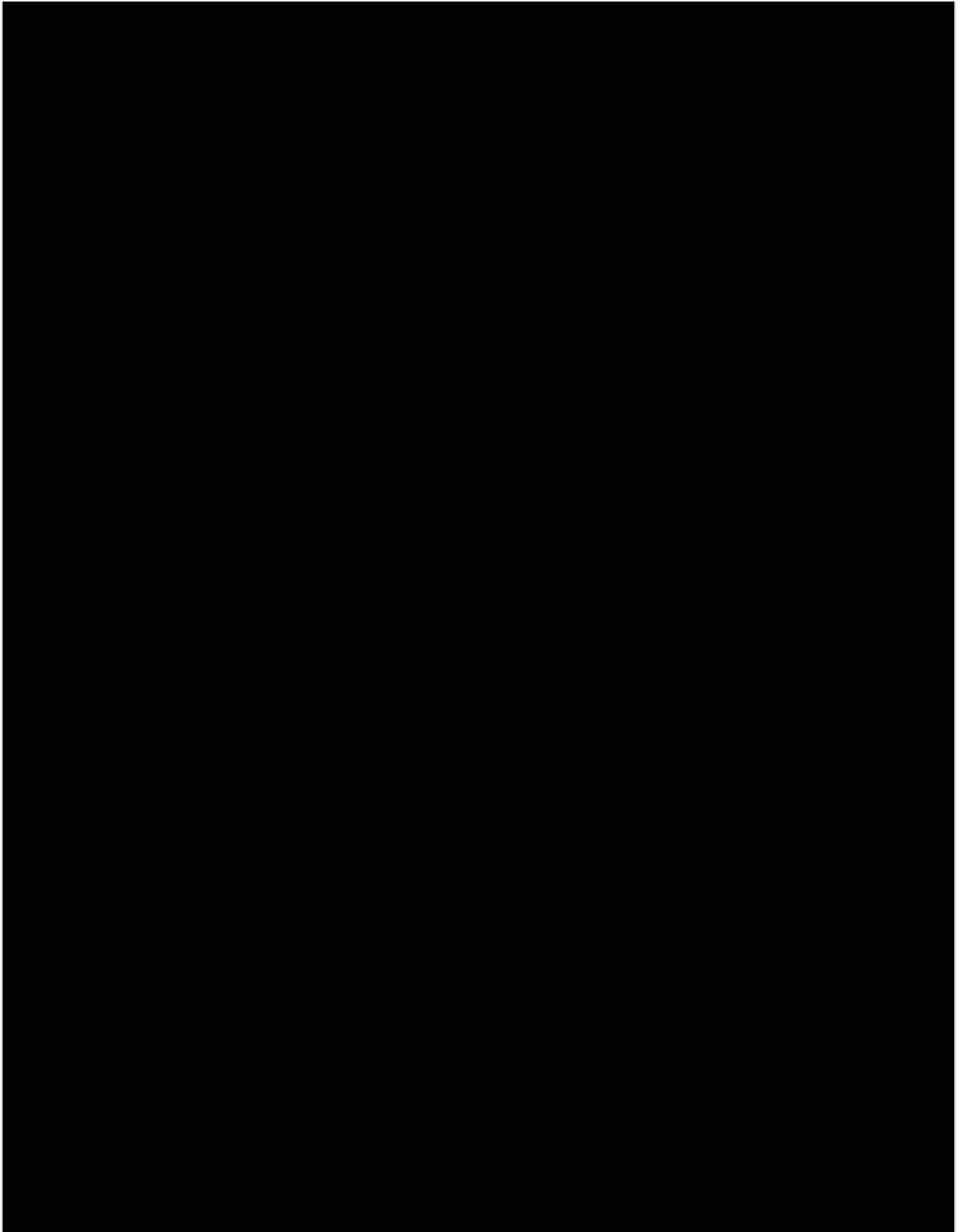




## Matlab Simulink Model



## Arduino Code for Barometric Sensor





## Bibliography

- [1] *Water Rocket Simulator*. (2024, May 20). Retrieved from Air Command Water Rockets:  
<http://www.aircommandrockets.com/sim/simulator.htm>
- [2] (2024, March 15). Retrieved from Airfoil Tools: <http://airfoiltools.com/>
- [3] *ISO 2533:1975*. (1975). Retrieved from International Standard Organization:  
<https://www.iso.org/standard/7472.html>
- [4] Podesta, M. d. (2007). *A guide to building and understanding the physics of Water Rockets*. National Physical Laboratory.
- [5] *Styrofoam™ Brand Highload*. (2024, May 10). Retrieved from DuPont:  
<https://www.dupont.com/products/styrofoam-brand-highload.html>
- [6] (2024, March 15). Retrieved from Airfoil Tools: <http://airfoiltools.com/>
- [7] Dodge, F. T. (2000). *THE NEW “DYNAMIC BEHAVIOR OF LIQUIDS IN MOVING CONTAINERS”*. Southwest Research Institute.
- [8] Makes, M. (2023, November 1). Cura Infill Settings Guide: Optimize Strength & Save Time — Modern Makes. Modern Makes. <https://www.modernmakes.ca/3d-printing/cura-infill-settings-guide>